

Gradient Estimation for Binary Latent Variables via Gradient Variance Clipping

Russell Z. Kunes^{1,2,4}, Mingzhang Yin^{4,5}, Max Land², Doron Haviv², Dana Pe'er^{2,3}, Simon Tavaré^{1,4}

¹Department of Statistics, Columbia University

²Computational and Systems Biology, Memorial Sloan Kettering Cancer Center

³Howard Hughes Medical Institute

⁴Irving Institute of Cancer Dynamics, Columbia University

⁵Warrington College of Business, University of Florida

Abstract

Gradient estimation is often necessary for fitting generative models with discrete latent variables, in contexts such as reinforcement learning and variational autoencoder (VAE) training. The DisARM estimator (Yin et al. 2020; Dong, Mnih, and Tucker 2020) achieves state of the art gradient variance for Bernoulli latent variable models in many contexts. However, DisARM and other estimators have potentially exploding variance near the boundary of the parameter space, where solutions tend to lie. To ameliorate this issue, we propose a new gradient estimator *bitflip-1* that has lower variance at the boundaries of the parameter space. As *bitflip-1* has complementary properties to existing estimators, we introduce an aggregated estimator, *unbiased gradient variance clipping* (UGC) that uses either a *bitflip-1* or a DisARM gradient update for each coordinate. We theoretically prove that UGC has uniformly lower variance than DisARM. Empirically, we observe that UGC achieves the optimal value of the optimization objectives in toy experiments, discrete VAE training, and in a best subset selection problem.

Introduction

Many modern machine learning tasks rely on stochastic gradient estimators, where the estimand is the gradient of an expected value $\mathbb{E}_{\mathbf{z} \sim p(\mathbf{z}; \theta)}[f(\mathbf{z})]$ that is intractable to compute (Mohamed et al. 2020). For example, in reinforcement learning it is often of interest to compute the gradient of an expected reward with respect to the parameters of a distribution over actions, where the reward may be a black box function of discrete states and actions (Li 2017). In variational inference, the objective function is the evidence lower bound, expressed as an expected value of the log joint probability of latent variable and data under a variational distribution (Ranganath, Gerrish, and Blei 2014; Blei, Kucukelbir, and McAuliffe 2017). In many cases \mathbf{z} is discrete; for example, in the design of biological sequences (Brookes, Park, and Listgarten 2019) or in models with spike and slab Bayesian priors (Moran et al. 2021).

When the latent variables \mathbf{z} are discrete and high dimensional, there are several challenges in optimizing the

mean-valued objective with respect to the distributional parameters θ . First, computing the exact expectation often requires an intractable number of function evaluations due to an exponential number of summation terms (AUEB, Lázaro-Gredilla et al. 2015a). Moreover, the derivative of the function itself with respect to discrete variables is not well defined so the chain rule-based reparametrization trick (Kingma and Welling 2013) cannot be used.

A number of methods for estimating the gradient of expected values with respect to discrete random variables have been devised (Dong, Mnih, and Tucker 2020; Dimitriev and Zhou 2021; Dong, Mnih, and Tucker 2021; Yin, Yue, and Zhou 2019; AUEB, Lázaro-Gredilla et al. 2015b; Tucker et al. 2017; Grathwohl et al. 2017; Titsias and Shi 2022a). A central role shared among the designs of useful gradient estimation is to control the bias and variance of the estimates. One line of research reduces the gradient variance in a trade-off of introducing bias. Widely used methods include continuous relaxations such as the Gumbel-softmax trick (Jang, Gu, and Poole 2016; Maddison, Mnih, and Teh 2016; Paulus et al. 2020), and the straight through gradient estimator (Yin et al. 2019), which have been successfully applied for learning latent representations of images (Razavi, Van den Oord, and Vinyals 2019) and text (Tran et al. 2019). Another line of work considers unbiased estimates that offer guarantees of convergence under conditions on the learning rate sequence (Ranganath, Gerrish, and Blei 2014; Robbins and Monro 1951). Some methods construct control variate baselines by continuous relaxation of the discrete distributions (Tucker et al. 2017; Grathwohl et al. 2017), by first-order Taylor expansions (Gu et al. 2015; Titsias and Shi 2022b), or by Stein operators (Shi et al. 2022). Other methods reduce the estimator variance by applying antithetic sampling and coupled sampling (Yin and Zhou 2018; Dong, Mnih, and Tucker 2020; Dimitriev and Zhou 2021; Yin, Yue, and Zhou 2019; Yin et al. 2020; Kool, van Hoof, and Welling 2019). Our work proceeds in this direction of designing unbiased and low-variance gradient estimators for discrete optimization.

In this work, we notice that in the context of Bernoulli discrete latent variables, a number of existing unbiased methods have unfavorably high variance at the boundary of the parameter space (namely, near 0 and near 1) due to reliance on an importance weight that is necessary in order to

maintain unbiasedness. To address this downside of existing estimators, we introduce an *unbiased gradient variance clipping* (UGC) estimator that sidesteps this issue by conditionally using one of two types of gradient estimators. For a given coordinate, when values of the probability parameter θ are near $\frac{1}{2}$, UGC updates the parameter values in the direction of the DisARM gradient estimate. On the other hand, when values of the probability θ become close to the boundary, UGC transitions to using a novel gradient estimator, *bitflip-1*, that has *complementary* properties to existing estimators that require $O(1)$ function evaluations. Namely, rather than considering coordinate-wise independent samples of \mathbf{z} , bitflip-1 updates only a single coordinate of the parameter vector at a time, while holding other coordinates fixed to minimize variance. The result is that bitflip-1 has variance linear in the latent dimension K but without explicit dependence on the latent Bernoulli parameters. Our proposed estimator, UGC, has guaranteed uniformly lower variance than DisARM and is robust across practical problems where either DisARM or bitflip-1 alone may fail.

Background

Consider the problem of estimating the gradient:

$$\nabla_{\theta} \mathbb{E}_{p(\mathbf{z}; \theta)} [f(\mathbf{z})] \quad (1)$$

where $\mathbf{z} = (z_1, \dots, z_K)$, $z_i \sim \text{Bernoulli}(\theta_i)$, $\theta_i \in [0, 1]$, independently, $p(\mathbf{z}; \theta) = \prod_{i=1}^K \text{Bernoulli}(\theta_i)$, and f is a potentially complicated and nonlinear function with domain on the lattice. This problem arises in discrete latent variable modeling and reinforcement learning. To compute the exact gradient, we can replace the expectation in Equation (1) with the summation over all possible values of \mathbf{z} which has 2^K summation terms. Computing the exact gradient thus requires an exponential number of evaluations which is infeasible to compute per iteration of gradient descent in high dimensional problems. Specifically we focus on the context of Bernoulli VAEs where $p_{\lambda}(\mathbf{x}_i | \mathbf{z}_i)$ is parameterized by a neural network, while $\mathbf{z} \in \{0, 1\}^K$, and we fit an encoder network $q_{\theta}(\mathbf{z} | \mathbf{x})$ to maximize the evidence lower bound (ELBO):

$$\mathcal{L}(\theta, \lambda) = \mathbb{E}_q \{ \log p_{\lambda}(\mathbf{x} | \mathbf{z}) + \log p(\mathbf{z}) - \log q_{\theta}(\mathbf{z} | \mathbf{x}) \}.$$

The exact gradient of the objective function with respect to θ involves 2^k terms in general. As a result, we are forced to use a stochastic estimate of the gradient. Two methods are commonly applied for this task; score function gradient estimators (Ranganath, Gerrish, and Blei 2014), and the reparameterization trick (Kingma and Welling 2013).

The score function gradient estimator

The score function gradient estimator (also called Reinforce) is $\hat{g} := f(\mathbf{z}) \nabla \log p(\mathbf{z}; \theta)$. Its unbiasedness follows from the following computation, assuming the conditions

of the dominated convergence theorem holds for f :

$$\begin{aligned} \nabla_{\theta} \mathbb{E}_{p(\mathbf{z}; \theta)} [f(\mathbf{z})] &= \int f(\mathbf{z}) \nabla_{\theta} p(\mathbf{z}; \theta) d\mu(\mathbf{z}) \\ &= \int f(\mathbf{z}) \nabla_{\theta} (\log p(\mathbf{z}; \theta)) p(\mathbf{z}; \theta) d\mu(\mathbf{z}) \\ &= \mathbb{E} \left\{ f(\mathbf{z}) \nabla_{\theta} \log p(\mathbf{z}; \theta) \right\}. \end{aligned}$$

The estimator is generally applicable but in many cases has too high variance to be useful in practice. However, this estimator has proven useful in many situations with the inclusion of variance reduction techniques such as control variates (Ranganath, Gerrish, and Blei 2014; Tucker et al. 2017; Grathwohl et al. 2017).

The ARM and DisARM gradient estimators

ARM (Yin and Zhou 2018) and DisARM (also called U2G) (Dong, Mnih, and Tucker 2020; Yin et al. 2020) are two methods for reducing the variance of the score function gradient estimator for Bernoulli latent variables. As notation, α_{θ} will refer to the logits of the Bernoulli parameter, i.e. $\alpha_{\theta} := \log \frac{\theta}{1-\theta}$. The ARM estimator is motivated by a reparameterization. In one dimension, letting $b \sim \text{Logistic}(\alpha_{\theta}, 1)$ and $z = \mathbf{1}_{b>0}$; the desired gradient $\nabla_{\theta} \mathbb{E} [f(z)] = \nabla_{\theta} \mathbb{E}_b [f(\mathbf{1}_{b>0})] = \mathbb{E}_b [f(\mathbf{1}_{b>0}) \nabla_{\theta} \log q_{\theta}(b)]$ where q_{θ} is the likelihood of the Logistic distribution with parameter α_{θ} . Logistic random variables with identical marginal distributions can be sampled by letting $\epsilon \sim \text{Logistic}(0, 1)$ and setting $b = \epsilon + \alpha_{\theta}$ and $\tilde{b} = -\epsilon + \alpha_{\theta}$. This antithetic sampling produces an estimator with reduced variance:

$$\begin{aligned} \hat{g}_{\text{ARM}} &:= \frac{1}{2} (f(\mathbf{1}_{b>0}) \nabla_{\theta} \log q_{\theta}(b) + f(\mathbf{1}_{\tilde{b}>0}) \nabla_{\theta} \log q_{\theta}(\tilde{b})) \\ &= \frac{1}{2} (f(\mathbf{1}_{b>0}) - f(\mathbf{1}_{\tilde{b}>0})) \nabla_{\theta} \log q_{\theta}(b) \\ &= (f(z) - f(\tilde{z})) (u - \frac{1}{2}) \nabla_{\theta} \alpha_{\theta}. \end{aligned}$$

Here, $\sigma(\cdot)$ is the sigmoid operation and, u is a uniform random variable defined by $\sigma(b - \alpha_{\theta})$, and $z = \mathbf{1}_{1-u < \theta}$, $\tilde{z} = \mathbf{1}_{u < \theta}$. The procedure naturally extends to the multi-dimensional case giving the estimator $\hat{g}_{\text{ARM}} = ((f(\mathbf{z}) - f(\tilde{\mathbf{z}}))(\mathbf{u} - \frac{1}{2})) \nabla_{\theta} \alpha_{\theta}$

The DisARM estimator takes a conditional expectation of the ARM estimator, conditioning on the values (z, \tilde{z}) :

$$\begin{aligned} \hat{g}_{\text{DisARM}} &= \mathbb{E}_{p(b|z, \tilde{z})} [\hat{g}_{\text{ARM}}] \\ &= \frac{1}{2} (f(z) - f(\tilde{z})) (-1)^{\tilde{z}} \mathbf{1}_{z \neq \tilde{z}} \sigma(|\alpha_{\theta}|) \nabla_{\theta} \alpha_{\theta} \end{aligned}$$

This extends to the multi-dimensional case in an analogous way, requiring a constant number of function evaluations, and also further reduces the variance of ARM estimator by nature of Rao-Blackwellization.

Variance properties of DisARM at the boundary

Though DisARM is competitive compared to existing methods of gradient estimation, it has unfavorable variance at the

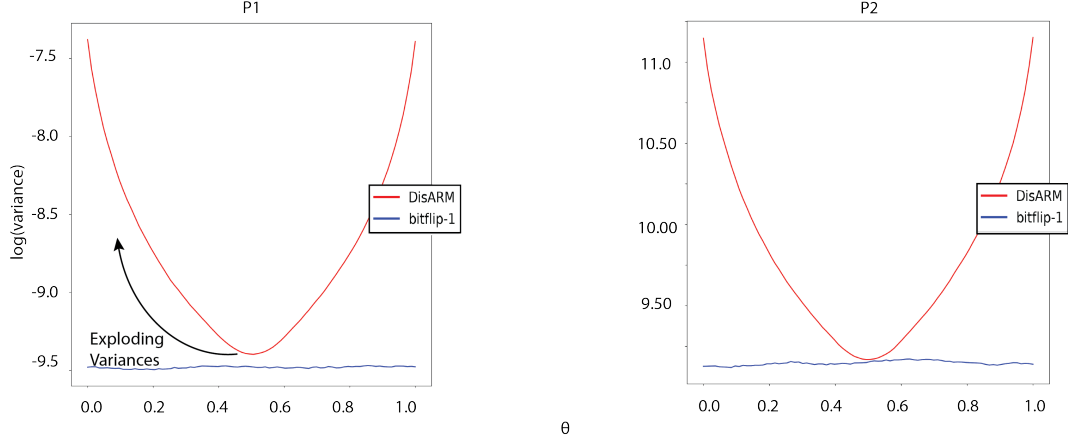


Figure 1: DisARM gradient variances potentially explode at the boundary of parameter space. *Left*: variance curves for P1, $f(z) = \sum_{i=1}^K (z_i - t)^2$ *Right*: variance curves for P2 $f(z) = (\sum_{i=1}^K z_i - t)^2$. In both cases $K = 20$, with $\theta_1 = \dots \theta_{19} = 0.5$ and θ_{20} varying on the x-axis.

boundaries of the parameter space. Reparameterizing the DisARM estimator in terms of probability θ gives:

$$\hat{g}_{DisARM,j} = \frac{1}{2} (f(\mathbf{z}) - f(\tilde{\mathbf{z}})) \frac{1}{\min(\theta_j, 1 - \theta_j)} \mathbf{1}_{z_j \neq \tilde{z}_j} (-1)^{\tilde{z}_j}$$

where \tilde{z}_j satisfies $\mathbb{P}[z_j = 0, \tilde{z}_j = 1] = \mathbb{P}[z_j = 1, \tilde{z}_j = 0] = \min(\theta_j, 1 - \theta_j)$, and $\mathbb{P}[z_j = \tilde{z}_j] = |1 - 2\theta_j|$.

We analyze the variance as the difference $\mathbb{E}[(\hat{g}_{DisARM,j})^2] - \mathbb{E}[(\hat{g}_{DisARM,j})]^2$. Without loss of generality, considering the case where $\theta_j < \frac{1}{2}$, the expected square $\mathbb{E}[(\hat{g}_{DisARM,j})^2]$ is:

$$\mathbb{E}\left[\frac{1}{4} (f(\mathbf{z}) - f(\tilde{\mathbf{z}}))^2 \frac{1}{\theta_j^2} \mathbf{1}_{z_j \neq \tilde{z}_j}\right] = \frac{1}{2\theta_j} \mathbb{E}\left[(f(\mathbf{z}_1^{(j)}) - f(\tilde{\mathbf{z}}_0^{(j)}))^2\right] \quad (2)$$

where $\mathbf{z}_1^{(j)}$ and $\tilde{\mathbf{z}}_0^{(j)}$ are defined by hard-coding the j 'th element of \mathbf{z} as 1 and 0 respectively and sampling remaining shared elements from their respective distributions. For unbiased gradient estimators, the term $\mathbb{E}[\hat{g}]^2 = (\mathbb{E}[f(\mathbf{z})|z_j = 1] - \mathbb{E}[f(\mathbf{z})|z_j = 0])^2$ are the same. Therefore, Equation (2) suggests that DisARM suffers from large variances when $\theta_j \approx 1$ or $\theta_j \approx 0$ (see Figure 1). Another estimator competitive with DisARM is Reinforce-loo (Kool, van Hoof, and Welling 2019), expressed as $\frac{1}{2\theta_j(1-\theta_j)} \left((f(z_{1,j}) - f(z_{2,j}))(z_{1,j} - \theta_j) + (f(z_{2,j}) - f(z_{1,j}))(z_{2,j} - \theta_j) \right)$ where now \mathbf{z}_1 and \mathbf{z}_2 are sampled independently. Again, the presence of the $\frac{1}{2\theta_j(1-\theta_j)}$ weight induces high variances at the boundary. This motivates us to consider estimators with bounded variance at the boundary. However, we note that this problem might be ameliorated by parameterizing θ by logits $\theta = \frac{e^\phi}{1+e^\phi}$ with $\nabla_\phi \theta = \theta(1 - \theta)$ as is commonly done in practice. Though this parameterization avoids explicit enforcement of the $[0,1]$ constraint during optimization, solutions at the boundary

cannot be reached exactly. In our simulations, we have observed slower convergence of this approach relative to projected gradient descent in a number of problem settings.

Unbiased Monte Carlo estimate of the gradient via bit flips

Note that the exact gradient is given by $E[f(\mathbf{z})|z_j = 1] - E[f(\mathbf{z})|z_j = 0]$. This suggests a simple estimation scheme: sample $\mathbf{z} \sim p_\theta$, and let $\tilde{\mathbf{z}}^{(j)}$ be the vector where the j 'th element of \mathbf{z} is flipped. The single sample estimate is then $(-1)^{z_j} (f(\tilde{\mathbf{z}}^{(j)}) - f(\mathbf{z}))$. We can apply this to all elements of the gradient for a single sample \mathbf{z} and retain the unbiasedness property. Since this requires $O(K)$ function evaluations with K as the dimension of variable \mathbf{z} , which may be too expensive in many settings, we define and analyze *bitflip-1* as the randomized estimator given by sampling $\mathbf{z} \sim p_\theta$, sampling a random coordinate $j \sim \text{Categorical}(1, \dots, K)$, and setting the estimate $\hat{g}_{\text{bitflip-1},j} := K * (-1)^{z_j} (f(\tilde{\mathbf{z}}^{(j)}) - f(\mathbf{z}))$, $\hat{g}_{\text{bitflip-1},-j} := 0$. Interestingly, the only dependence of \hat{g} on θ is through the sampling procedure. We also point out that though the DisARM estimator is shown to be uniformly minimum variance among estimators that employ linear combinations of antithetic sampled Bernoulli variables ((Yin et al. 2020), Proposition 2), *bitflip-1* cannot be expressed in this manner (and moreover, the coordinates are no longer independent) and so is not dominated. In fact, *bitflip-1* is lower variance than DisARM whenever $\frac{1}{2 \min(\theta, 1-\theta)} > K$.

The expression of the gradient also suggests an interpretation of the DisARM estimator: that is, DisARM estimates $\mathbb{E}[f(\mathbf{z})|z_j = 1] - \mathbb{E}[f(\mathbf{z})|z_j = 0]$ with two samples and a multiplicative weight that ensures the unbiasedness property. Each of the two samples has j 'th coordinate that is marginally Bernoulli(θ_j), with a joint distribution between the two samples that gives us maximal amount of information about the gradient. If we are limited to two func-

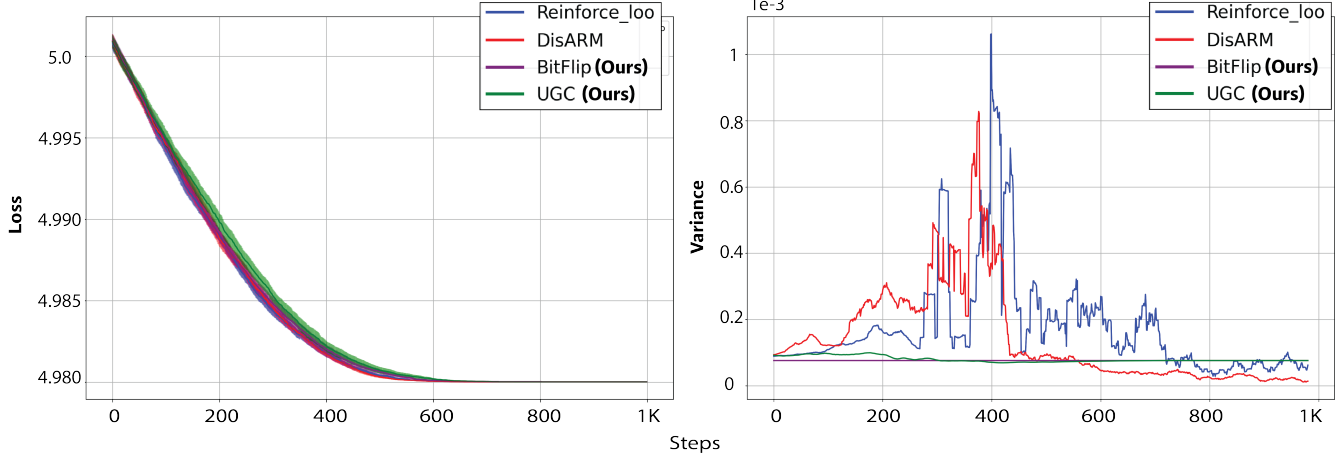


Figure 2: Performance on (P1) optimization problem min with $t = 0.499$, $K = 20$. All methods tested converge to the optimal solution in this setting, though DisARM and Reinforce-loo suffer higher gradient variances. *Left*: Training loss curves averaged over 10 trials for the (P1) optimization problem with error bars $\pm\sigma/\sqrt{10}$ *Right*: Gradient variances on (P1) averaged over 10 trials.

tion evaluations, this suggests considering estimates of the form $f(\mathbf{z}) - f(\tilde{\mathbf{z}})$ for some $(\mathbf{z}, \tilde{\mathbf{z}})$ with the marginal distribution $z_j \sim \text{Bernoulli}(\theta_j)$. However, with just two function evaluations it makes sense to disregard terms where $z_j = \tilde{z}_j$ as it is not clear how to construct an estimator of $\mathbb{E}[f(\mathbf{z})|z_j = 1] - \mathbb{E}[f(\mathbf{z})|z_j = 0]$ in these cases.

All of this suggests considering estimators of the form:

$$\hat{g}_j := (-1)^{\tilde{z}_j} [f(\mathbf{z}) - f(\tilde{\mathbf{z}})] \quad (3)$$

$$\times \frac{1}{p[z_j = 1, \tilde{z}_j = 0] + p[z_j = 0, \tilde{z}_j = 1]} \mathbf{1}_{z_j \neq \tilde{z}_j} \quad (4)$$

where the correction term (Eq. 4) is to retain unbiasedness. This recovers DisARM when $p[z_j = 1, \tilde{z}_j = 0] = p[z_j = 0, \tilde{z}_j = 1] = \min(\theta, 1 - \theta)$ and Reinforce-loo when $\mathbf{z} \perp\!\!\!\perp \tilde{\mathbf{z}}$. An important fact about DisARM is that it maximizes $p[z_j = 0, \tilde{z}_j = 1] + p[z_j = 1, \tilde{z}_j = 0]$, i.e. the coupling given by $p[z_j = 0, \tilde{z}_j = 1] = \min(\theta_j, 1 - \theta_j)$ has the highest probability of differing values between \tilde{z}_j and z_j subject to the marginal constraint that each random variable is Bernoulli(θ_j). This is due to the fact that $p[z_j = 0, \tilde{z}_j = 1] \leq \theta$ and $p[z_j = 0, \tilde{z}_j = 1] \leq 1 - \theta$ following the two constraints given by $p[z_j = 0] = p[z_j = 0, \tilde{z}_j = 1] + p[z_j = 0, \tilde{z}_j = 0]$ and $p[\tilde{z}_j = 1] = p[z_j = 1, \tilde{z}_j = 1] + p[z_j = 0, \tilde{z}_j = 1]$.

However, it is clear that the minimum variance coupling depends on f as we have:

$$E[\hat{g}^2] = \left(\frac{1}{p[z_j = 0, \tilde{z}_j = 1] + p[z_j = 1, \tilde{z}_j = 0]} \right) \quad (5)$$

$$\times \mathbb{E}((f(\mathbf{z}) - f(\tilde{\mathbf{z}}))^2 | z_j = 1, \tilde{z}_j = 0). \quad (6)$$

When f is continuous (in the sense that $|f(\mathbf{z}) - f(\tilde{\mathbf{z}})|$ is related to $d(\mathbf{z}, \tilde{\mathbf{z}})$ for a distance metric d) there is a trade-off between minimizing the first (Eq. 5) and second (Eq. 6)

terms. As $p[z_j = 0, \tilde{z}_j = 1]$ (and $p[z_j = 1, \tilde{z}_j = 0]$) increase, the expected function differences (Eq. 6) are likely to be large. If f is such that term (Eq. 6) tends to be large, independently sampled \mathbf{z} and $\tilde{\mathbf{z}}$ may even be lower variance than antithetic samples (Dong, Mnih, and Tucker 2020). DisARM updates the largest number of terms possible by maximizing the probabilities $p[z_j = 0, \tilde{z}_j = 1]$ and $p[z_j = 1, \tilde{z}_j = 0]$ and hence minimizes term (Eq. 5), but insodoing may incur high variance through large values of term (Eq. 6).

Variance properties of bitflip-1

Without loss of generality assume $\theta_i < 0.5$ and consider the variance of a single coordinate of each estimator. The argument can be easily extended to $\theta \geq 0.5$. We also assume the following natural continuity property of the function f :

Assumption 1. Given four binary vectors $z, w, \tilde{z}, \tilde{w} \in \{0, 1\}^K$, if $\{j : \tilde{z}_j \neq z_j\} \supset \{j : \tilde{w}_j \neq w_j\}$ and $w_i = z_i$ for all i such that $w_i = \tilde{w}_i$ and $z_i = \tilde{z}_i$, then $|f(w) - f(\tilde{w})| \leq |f(z) - f(\tilde{z})|$.

In other words, given two binary strings we cannot make their function evaluations closer by introducing additional coordinates where they differ. Since each estimator considered is unbiased, it suffices to consider $\mathbb{E}[\hat{g}^2]$ for each gradient estimator \hat{g} .

Proposition 1. (Variance of bitflip-1) Let \hat{g} be an estimator in the family of estimators given by (Eq. 3-4), which includes DisARM and Reinforce-loo gradient estimators. If Assumption 1 holds and if $\frac{1}{2 \min(\theta_j, 1 - \theta_j)} \geq K$:

$$\text{Var}(\hat{g}_{\text{bitflip-1}}) \leq \text{Var}(\hat{g})$$

We present an expanded version of this proposition and proof in the appendix. We also note that when $f(z)$ is separable, bitflip-1 has uniformly lower variance than DisARM in the following sense:

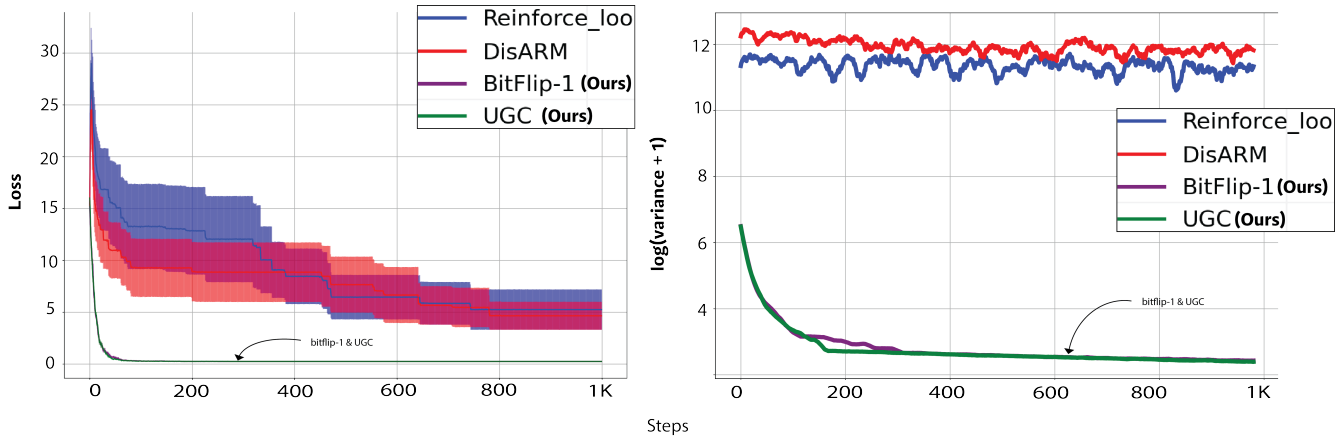


Figure 3: Performance on (P2) optimization problem with $t = 0.499$, $K = 20$. DisARM and Reinforce-loo frequently fail to converge, while experiencing high gradient variances. *Left*: Training loss curves averaged over 10 trials for the (P2) optimization problem with errors bars $\pm\sigma/\sqrt{10}$ *Right*: Average gradient variances on (P1) over 10 trials

Proposition 2. Consider a member of the family of estimators given by (Eq. 3-4), which includes DisARM and Reinforce-loo and denote this estimator \hat{g} . If $f(\mathbf{z}) = \sum_{i=1}^K h(z_i)$, then:

$$\min_{\theta_1, \dots, \theta_K} \max_{j=1, \dots, K} \text{Var}(\hat{g}_j) \geq \max_{\theta_1, \dots, \theta_K} \max_{j=1, \dots, K} \text{Var}(\hat{g}_{\text{bitflip}, j})$$

Unbiased Gradient Variance Clipping

Though bitflip-1 has bounded variance for a given latent variable dimension K , its variance grows linearly with K . Meanwhile, DisARM has variance growing with $\frac{1}{\min(\theta, 1-\theta)}$ despite only depending on K implicitly through the function f . Motivated by these complementary behaviors and fact that θ_j and K are available, we can construct an estimator that dominates DisARM as follows.

$$\hat{g}_{\text{UGC}, j} = \begin{cases} \hat{g}_{\text{bitflip}, j} & \text{if } \min(\theta_j, 1 - \theta_j) < \tau \\ \hat{g}_{\text{DisARM}, j} & \text{if } \min(\theta_j, 1 - \theta_j) \geq \tau \end{cases} \quad (7)$$

where τ is a tuning parameter of the estimator. We denote this estimator by *unbiased gradient variance clipping* (UGC) as it replaces potentially high variance gradient estimates with bounded variance estimates without breaking unbiasedness of the estimate. A standard choice of τ is $\frac{1}{2K}$, motivated by the following result:

Proposition 3. (Variance of UGC) Under assumption 1, when $\tau \leq \frac{1}{2K}$, $\text{Var}(\hat{g}^{(\text{UGC})}) \leq \text{Var}(\hat{g})$ for any \hat{g} in the family of estimators given by (Eq. 3-4), which includes DisARM and Reinforce-loo gradients.

We find that UGC achieves better performance than bitflip-1 and DisARM on a number of tasks.

Experiments

Toy experiments

In (Tucker et al. 2017), the authors optimize the objective $\mathbb{E}_\theta[(z - t)^2]$ where z is a single Bernoulli random variable

with a parameter θ and t is set to either 0.49 or 0.499. The optimizer of this problem is $\theta = 0$, with values of t closer to 0.5 representing harder problems. As bitflip-1 computes the exact gradient for univariate latent variable z , we extend this problem to two multivariate problems:

$$(P1) : \min \mathbb{E}[\sum_{k=1}^K (z_k - t)^2]; \quad (P2) : \min \mathbb{E}[(\sum_{k=1}^K z_k - t)^2]$$

In problem (P1), due to the separability of the objective, bitflip-1 computes the exact gradient multiplied by K and updates a random component (Figure 2). Problem (P2) is harder in the sense that it contains many interaction terms and the exact gradient is expensive to compute for moderate K . Figure 3 shows results for $K = 20$ and $t = 0.499$ (with other results in the appendix). Notably, for (P2) both the Reinforce-loo baseline and DisARM fail to converge to the optimum. This occurs due to the fact that these gradients can often be in the wrong direction due to noise and then are unable to estimate high magnitude gradients at $\theta = 1$. When $\theta \approx 1$, UGC will switch to using bitflip gradients and can move away from the suboptimal $\theta = 1$.

L_0 best subset regression

Fitting linear regression with a sparsity penalty has become a ubiquitous task across many domains (Tibshirani 2011). Such regression estimators frequently are computed by minimizing squared error subject to a constraint on the L_1 norm of the regression coefficients β . The non-convex problem of optimizing subject to constraint on the L_0 norm has received less attention due to computational challenges but is addressed in (Yin et al. 2020). Specifically, they consider the following estimator of β under the linear regression assumptions $y \sim \mathcal{N}(x^\top \beta, \sigma^2)$:

$$\min_{\beta} \frac{1}{n} \|\mathbf{y} - \mathbf{X}\beta\|_2^2 + \lambda \|\beta\|_0$$

This optimization problem penalizes the cardinality of the coefficient vector β , rather than its L_1 norm and so

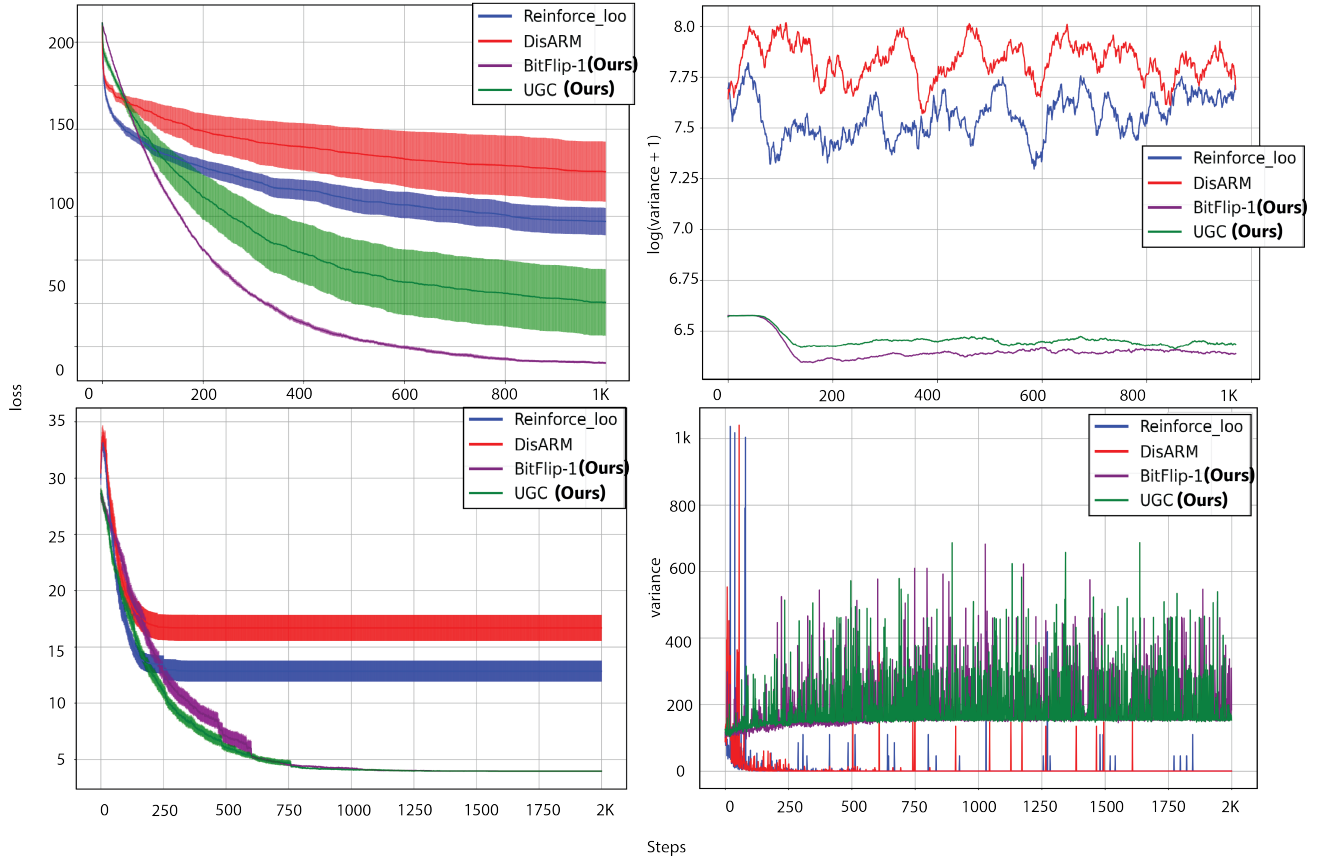


Figure 4: Performance on the gradient based subset optimization problem for linear regression. $p = 200$, $n = 60$, $\Sigma = I$, $|S| = 3$, *top*: $\text{SNR} = \beta^\top \beta / \sigma^2 = 3.8125$, parameterization by $\phi = \log(\theta / (1 - \theta))$ *bottom*: $\text{SNR} = \beta^\top \beta / \sigma^2 = 1.694$. Parameterization by θ , with projected gradient descent onto $[0, 1]$. *Left*: Training loss curves for the best subset optimization problem, averaged over 10 random samples of the data with error bars $\pm \sigma / \sqrt{10}$. *Right*: Average gradient variances across 10 random samples of the data. Though bitflip-1 and UGC are higher variance in the second example, we note that this is because they are in the correct part of parameter space

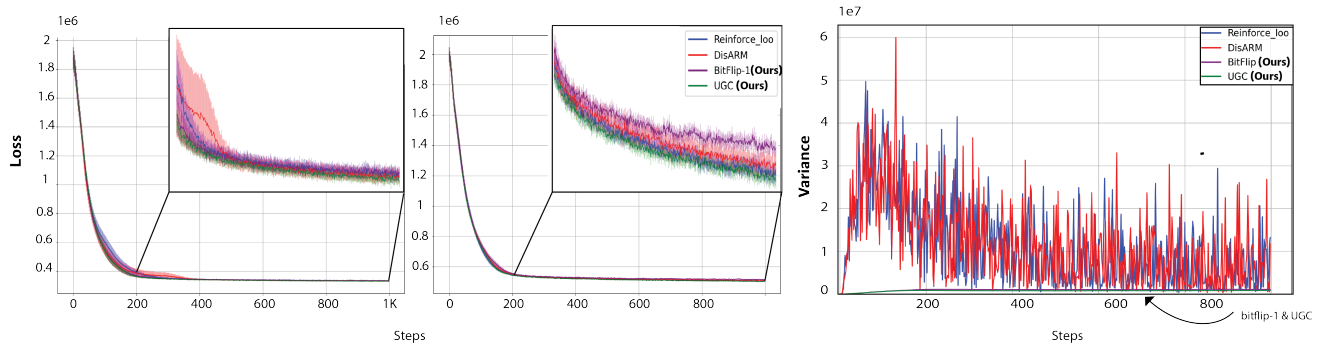


Figure 5: Performance on the gaussian mixture model problem fit via discrete variational autoencoders. Cluster means are sampled $N(0, 8^2)$ per simulation. *Right*: Training loss curves for the gaussian mixture model problem ($\sigma = 2.0$), averaged over 10 random samples of the data with error bars $\pm \sigma / \sqrt{10}$. *Middle*: Training loss curves for $\sigma = 4.0$ *Right*: Average gradient variances ($\sigma = 4.0$) across 10 random samples of the data. Through the experiment, the true number of clusters is 6, the number of features is 20, and the hidden dimension is 10

more directly encodes the assumption that the true coefficient vector is sparse. In (Yin et al. 2020), the authors show

that this problem can be approximately solved with the gradient estimator DisARM via the equivalent optimization

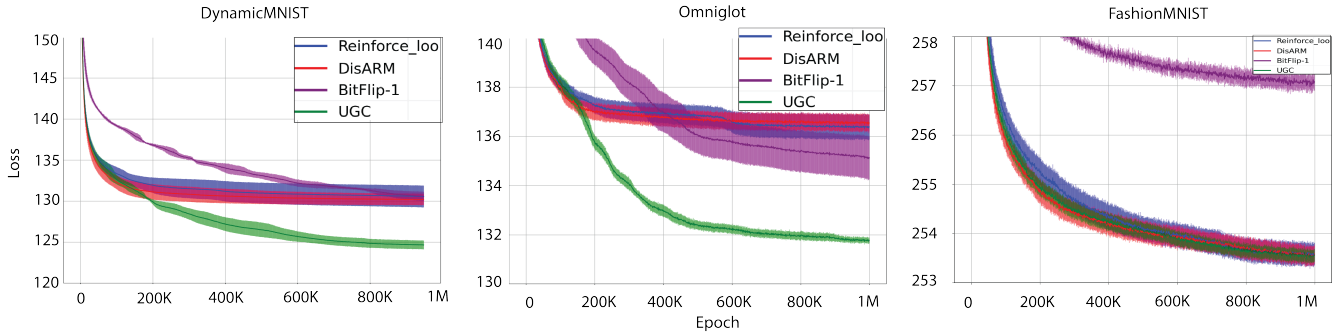


Figure 6: Performance on the binarized discrete VAE fit to DynamicMNIST, FashionMNIST and Omniglot datasets over 5 random seeds, with error bars given by $\pm\sigma/\sqrt{5}$. The binary latent variable is 30 dimensional with 1-layer encoder and decoder networks. UGC achieves better convergence than alternative estimators.

Table 1: False Positive Rate (FPR) of best subset selection.

SNR	Gradient estimator			
	bitflip-1	UGC	DisARM	Rein.-loo
15.25	0.0 (0.0)	0.0 (0.0)	0.05 (0.02)	0.04 (0.01)
3.81	0.0 (0.0)	0.0 (0.0)	0.06 (0.03)	0.04 (0.01)
1.69	0.01 (0.01)	0.01 (0.01)	0.06 (0.03)	0.05 (0.02)
0.95	0.04 (0.01)	0.03 (0.01)	0.06 (0.02)	0.05 (0.01)

Table 2: True Positive Rate (TPR) of best subset selection.

SNR	Gradient estimator			
	bitflip-1	UGC	DisARM	Rein.-loo
15.25	0.96 (0.1)	0.96 (0.1)	0.56 (0.26)	0.6 (0.36)
3.81	1.0 (0.0)	1.0 (0.0)	0.66 (0.26)	0.53 (0.16)
1.69	0.83 (0.27)	0.87 (0.22)	0.43 (0.26)	0.50 (0.31)
0.95	0.43 (0.30)	0.67 (0.21)	0.40 (0.29)	0.43 (0.21)

problem: $\min_{\theta} \mathbb{E}_{z \sim \theta} [\min_{\beta} \frac{1}{n} \|\mathbf{y} - \mathbf{X}(\mathbf{z} \odot \beta)\|_2^2 + \lambda \|\mathbf{z}\|_0]$ where \odot means elementwise multiplication. The solutions of the second problem are guaranteed to occur at the boundaries of the parameter space and coincide with the solution of the original regression problem. As the solutions occur at the boundary, this scenario is one where bitflip-1 and UGC perform well, shown in Figure 4. Specifically, in low signal-to-noise (SNR) settings, other gradient estimators cannot reliably recover the correct solution (Tables 1 and 2).

Gaussian mixture model

We investigate the capability of a discrete variational autoencoder fit with each gradient estimator to identify Gaussian mixtures. Specifically we generate samples from a 20-dimensional Gaussian mixture model distribution with 6 components by first sampling component means from a $N(0, 8^2)$ distribution, then sampling data conditional on component means from a Normal distribution with variance σ^2 , with σ^2 being the parameter controlling the signal to noise ratio. Though each estimator achieves comparable

convergence rate for multiple signal to noise ratios, bitflip-1 and UGC have markedly lower variance throughout training (Figure 5).

Discrete variational autoencoder training

We replicate the discrete variational autoencoder architecture and experimental setup on binarized DynamicMNIST, Omniglot and FashionMNIST datasets from (Yin and Zhou 2018) and (Dong, Mnih, and Tucker 2020). Interestingly, we note that DisARM exhibits fast convergence early on in training but later in training is unable to make progress, while bitflip-1 proceeds slowly during initial training but reaches a better final optimum. UGC achieves the best of both worlds: after switching to bitflip-1 derived gradients, it reaches a better solution than both methods (Figure 6).

Discussion

We have presented a method for producing low variance gradient estimates at the boundary of the parameter space for Bernoulli latent variable models. Noticing that existing methods suffer high variance gradients near the boundary of $[0, 1]$, we introduce a combined estimator, UGC, that uses DisARM gradients near the middle of $[0, 1]$ and bitflip-1 gradients near the boundary. We expect our approach to be useful for fitting various kinds of sparse latent variable models; for example, for fitting variational autoencoders with spike and slab priors via mean field variational inference (Moran et al. 2021). Our empirical results hopefully open the door to a number of theoretical questions. Future work may define classes of discrete functions and estimators where we can find optimal gradient estimators subject to constraint on the number of function evaluations.

References

- AUEB, T. R.; Lázaro-Gredilla, M.; et al. 2015a. Local expectation gradients for black box variational inference. *Advances in neural information processing systems*, 28.
- AUEB, T. R.; Lázaro-Gredilla, M.; et al. 2015b. Local expectation gradients for black box variational inference. *Advances in neural information processing systems*, 28.
- Blei, D. M.; Kucukelbir, A.; and McAuliffe, J. D. 2017. Variational inference: A review for statisticians. *Journal of the American statistical Association*, 112(518): 859–877.
- Brookes, D.; Park, H.; and Listgarten, J. 2019. Conditioning by adaptive sampling for robust design. In *International conference on machine learning*, 773–782. PMLR.
- Dimitriev, A.; and Zhou, M. 2021. Arms: Antithetic-reinforce-multi-sample gradient for binary variables. In *International Conference on Machine Learning*, 2717–2727. PMLR.
- Dong, Z.; Mnih, A.; and Tucker, G. 2020. DisARM: An antithetic gradient estimator for binary latent variables. *Advances in neural information processing systems*, 33: 18637–18647.
- Dong, Z.; Mnih, A.; and Tucker, G. 2021. Coupled gradient estimators for discrete latent variables. *Advances in Neural Information Processing Systems*, 34: 24498–24508.
- Grathwohl, W.; Choi, D.; Wu, Y.; Roeder, G.; and Duvenaud, D. 2017. Backpropagation through the void: Optimizing control variates for black-box gradient estimation. *arXiv preprint arXiv:1711.00123*.
- Gu, S.; Levine, S.; Sutskever, I.; and Mnih, A. 2015. Muprop: Unbiased backpropagation for stochastic neural networks. *arXiv preprint arXiv:1511.05176*.
- Jang, E.; Gu, S.; and Poole, B. 2016. Categorical reparameterization with gumbel-softmax. *arXiv preprint arXiv:1611.01144*.
- Kingma, D. P.; and Welling, M. 2013. Auto-encoding variational bayes. *arXiv preprint arXiv:1312.6114*.
- Kool, W.; van Hoof, H.; and Welling, M. 2019. Buy 4 reinforce samples, get a baseline for free! *ICLR 2019 workshop: Deep RL Meets Structured Prediction*.
- Li, Y. 2017. Deep reinforcement learning: An overview. *arXiv preprint arXiv:1701.07274*.
- Maddison, C. J.; Mnih, A.; and Teh, Y. W. 2016. The concrete distribution: A continuous relaxation of discrete random variables. *arXiv preprint arXiv:1611.00712*.
- Mohamed, S.; Rosca, M.; Figurnov, M.; and Mnih, A. 2020. Monte Carlo Gradient Estimation in Machine Learning. *Journal of machine learning research: JMLR*, 21(132): 1–62.
- Moran, G. E.; Sridhar, D.; Wang, Y.; and Blei, D. M. 2021. Identifiable variational autoencoders via sparse decoding. *arXiv preprint arXiv:2110.10804*.
- Naesseth, C.; Ruiz, F.; Linderman, S.; and Blei, D. 2017. Reparameterization gradients through acceptance-rejection sampling algorithms. In *Artificial Intelligence and Statistics*, 489–498. PMLR.
- Paulus, M.; Choi, D.; Tarlow, D.; Krause, A.; and Maddison, C. J. 2020. Gradient estimation with stochastic softmax tricks. *Advances in Neural Information Processing Systems*, 33: 5691–5704.
- Ranganath, R.; Gerrish, S.; and Blei, D. 2014. Black box variational inference. In *Artificial intelligence and statistics*, 814–822. PMLR.
- Razavi, A.; Van den Oord, A.; and Vinyals, O. 2019. Generating diverse high-fidelity images with vq-vae-2. *Advances in neural information processing systems*, 32.
- Robbins, H.; and Monroe, S. 1951. A stochastic approximation method. *The annals of mathematical statistics*, 400–407.
- Shi, J.; Zhou, Y.; Hwang, J.; Titsias, M. K.; and Mackey, L. 2022. Gradient Estimation with Discrete Stein Operators. *arXiv:2202.09497*.
- Tibshirani, R. 2011. Regression shrinkage and selection via the lasso: a retrospective. *Journal of the Royal Statistical Society: Series B (Statistical Methodology)*, 73(3): 273–282.
- Titsias, M.; and Shi, J. 2022a. Double Control Variates for Gradient Estimation in Discrete Latent Variable Models. In *International Conference on Artificial Intelligence and Statistics*, 6134–6151. PMLR.
- Titsias, M.; and Shi, J. 2022b. Double Control Variates for Gradient Estimation in Discrete Latent Variable Models. In Camps-Valls, G.; Ruiz, F. J. R.; and Valera, I., eds., *Proceedings of The 25th International Conference on Artificial Intelligence and Statistics*, AISTATS.
- Tran, D.; Vafa, K.; Agrawal, K.; Dinh, L.; and Poole, B. 2019. Discrete flows: Invertible generative models of discrete data. *Advances in Neural Information Processing Systems*, 32.
- Tucker, G.; Mnih, A.; Maddison, C. J.; Lawson, J.; and Sohl-Dickstein, J. 2017. Rebar: Low-variance, unbiased gradient estimates for discrete latent variable models. *Advances in Neural Information Processing Systems*, 30.
- Yin, M.; Ho, N.; Yan, B.; Qian, X.; and Zhou, M. 2020. Probabilistic best subset selection via gradient-based optimization. *arXiv preprint arXiv:2006.06448*.
- Yin, M.; Yue, Y.; and Zhou, M. 2019. ARSM: Augment-REINFORCE-swap-merge estimator for gradient backpropagation through categorical variables. In *International Conference on Machine Learning*, 7095–7104. PMLR.
- Yin, M.; and Zhou, M. 2018. Arm: Augment-reinforcemerge gradient for discrete latent variable models. *arXiv preprint arXiv:1807.11143*.
- Yin, P.; Lyu, J.; Zhang, S.; Osher, S.; Qi, Y.; and Xin, J. 2019. Understanding straight-through estimator in training activation quantized neural nets. *arXiv preprint arXiv:1903.05662*.

Supplementary Material

Further background: Reparameterization trick

Another gradient estimator is given by the reparameterization trick (Kingma and Welling 2013), which requires $f(\mathbf{z})$ to be differentiable, and for \mathbf{z} to be expressible as a differentiable transformation of exogenous noise $\mathbf{z} = T(\theta, \epsilon)$, where $\epsilon \sim g(\cdot)$ is free of θ . When this holds, an unbiased estimator of $\nabla \mathbb{E}_{p(\mathbf{z}; \theta)}[f(\mathbf{z})]$ is $\nabla_T f(T(\epsilon, \theta)) \left(\frac{\partial}{\partial \theta} T(\theta, \epsilon) \right)$, where the second term is the Jacobian matrix of the transformation. Unbiasedness follows from a change of variables: $\mathbb{E}_{p(\mathbf{z}; \theta)}[f(\mathbf{z})] = \mathbb{E}_\epsilon[f(T(\theta, \epsilon))]$, and then applying the chain rule. The reparameterization gradient estimator is lower variance than score function gradient estimator, but less generally applicable (Naesseth et al. 2017). In the context of discrete random variables, it's necessary to apply a continuous relaxation to \mathbf{z} and extend the domain of f to account for continuous input.

Exact gradient

The expression of the exact gradient as $\mathbb{E}[f(\mathbf{z})|z_j = 1] - \mathbb{E}[f(\mathbf{z})|z_j = 0]$ is seen as follows:

$$\begin{aligned} \nabla_{\theta_j} \mathbb{E}f(z_1, \dots, z_k) &= \sum_{\mathbf{z} \in \{0,1\}^k} f(z_1, \dots, z_k) \times \nabla_{\theta_j} \prod_{i=1}^k \theta_i^{z_i} (1 - \theta_i)^{1-z_i} \\ &= \sum_{\mathbf{z}: z_j=1} f(z_1, \dots, z_k) \prod_{i \neq j} \theta_i^{z_i} (1 - \theta_i)^{1-z_i} - \sum_{\mathbf{z}: z_j=0} f(z_1, \dots, z_k) \prod_{i \neq j} \theta_i^{z_i} (1 - \theta_i)^{1-z_i} \\ &= \mathbb{E}[f(\mathbf{z})|z_j = 1] - \mathbb{E}[f(\mathbf{z})|z_j = 0] \end{aligned}$$

Step up UGC procedure (tUGC)

Though UGC lowers the variance of DisARM, it is not the optimal aggregation procedure. This is due to the fact that the procedure is still unbiased if only a subset of the coordinates can be chosen to be updated. If we are choosing only a subset of the coordinates it makes sense to choose the smallest values of $\min(\theta_j, 1 - \theta_j)$ to be updated via bitflip-1 rather than DisARM, as these would have the highest variance DisARM gradients. Let $\tilde{\theta}_{(1)}, \dots, \tilde{\theta}_{(K)}$ be the sorted values of $\min(\theta_j, 1 - \theta_j)$ and $\sigma(\cdot)$ the reverse permutation. Consider $\hat{T} := \sup\{T : \tilde{\theta}_{(T)} \leq \frac{1}{2T}\}$. Sample $q \sim \text{Categorical}(1, \dots, \hat{T})$ and update $\hat{g}_{\sigma(q)} = \hat{T}[f(\mathbf{z}_1^{\sigma(q)}) - f(\mathbf{z}_0^{\sigma(q)})]$ with other \hat{g}_j corresponding to the \hat{T} lowest values of $\tilde{\theta}$ set to 0. The remaining indices corresponding to larger values of $\tilde{\theta}$ are set to the DisARM estimate. This is lower variance than UGC as $\hat{T} \leq K$. We denote this modification tUGC. After a few gradient updates, tUGC tends to behave like bitflip-1 (shown in Figure 7). However, these first few steps can be quite important (Figure 8-9) as tUGC vastly outperforms bitflip-1 for VAE training. As performance is quite similar to UGC overall we report results from UGC in the main text.

Proof of Proposition 1

We present an expanded version of the proposition statement. First we define the K -sample versions of each of the estimators as follows. For bitflip, $\hat{g}_{\text{bitflip-k},j} = f(\mathbf{z}_1^{(j)}) - f(\mathbf{z}_0^{(j)})$ (requiring $K+1$ function evaluations) and $\hat{g}_{\text{DisARM-k},j} = \frac{1}{K} \sum_{k=1}^K \hat{g}_{\text{DisARM},j}^{(k)}$ (with each $\hat{g}_{\text{DisARM},j}^{(k)}$ being an independently generated instance of the DisARM estimator). The definition of $\hat{g}_{\text{Reinforce-loo-k}}$ is analogous. The latter two estimators require $2K$ function evaluations.

Proposition 4. Assume that \hat{g} is an estimator of the gradient that can be expressed according to (Eq.3-4). and $\hat{g}_k := \frac{1}{K} \sum_{i=1}^K \hat{g}^{(i)}$ for independently generated $\hat{g}^{(i)}$. Under Assumption 1, we have:

- $\text{Var}(\hat{g}_{\text{bitflip-k}}) \leq \text{Var}(\hat{g})$
- $\text{Var}(\hat{g}_{\text{bitflip-k}}) \leq \text{Var}(\hat{g}_{\text{Reinforce}})$; if additionally $f \geq 0$ or $f \leq 0$

If $\frac{1}{2 \min(\theta_j, 1 - \theta_j)} \geq K$:

- $\text{Var}(\hat{g}_{\text{bitflip-1}}) \leq \text{Var}(\hat{g})$
- $\text{Var}(\hat{g}_{\text{bitflip-k}}) \leq \text{Var}(\hat{g}_k)$
- $\text{Var}(\hat{g}_{\text{bitflip-1}}) \leq \text{Var}(\hat{g}_{\text{Reinforce}})$; if additionally $f \geq 0$ or $f \leq 0$

Proof. The bitflip- K estimator for $\nabla_{\theta_j} \mathbb{E}[f(\mathbf{z})]$ is:

$$\hat{g}_{\text{bitflip-K},j} := f(\mathbf{z}_1^{(j)}) - f(\mathbf{z}_0^{(j)})$$

while the bitflip-1 estimator is

$$\hat{g}_{\text{bitflip-1}} := K * (f(\mathbf{z}_1^{(j)}) - f(\mathbf{z}_0^{(j)})) \mathbf{1}_{q=j}$$

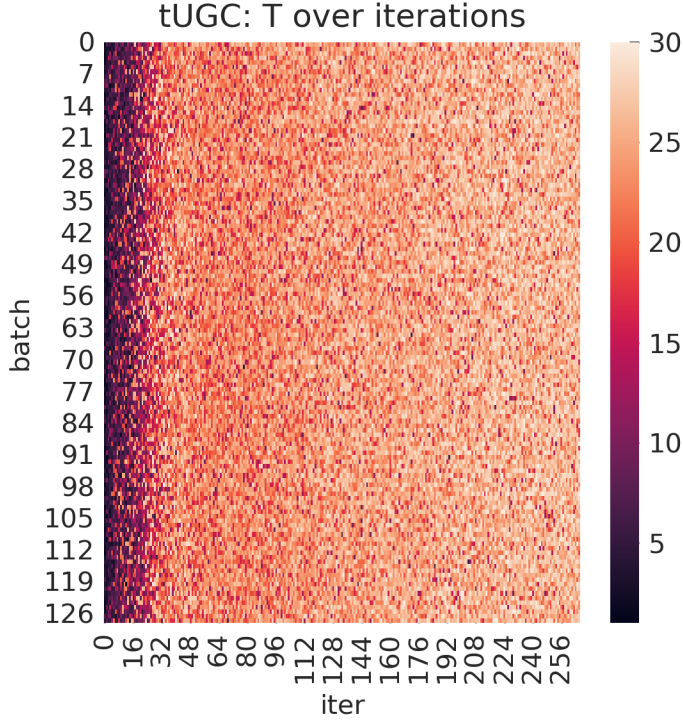


Figure 7: Convergence of tUGC to bitflip-1 over stochastic gradient descent iterations. Here, $K = 30$ and the value of \hat{T} approaches K for each coordinate

where $\mathbf{z} \sim p_\theta$ is a sample from the given factorial Bernoulli distribution, $\mathbf{z}_1^{(j)}$ is \mathbf{z} with its j 'th element set to 1, $\mathbf{z}_0^{(j)}$ has its j 'th element set to 0, and $q \sim \text{Categorical}(1, \dots, K)$. For the first claim, we consider the bitflip K -sample estimator:

$$\begin{aligned} \mathbb{E}[\hat{g}_j^2] &= \frac{1}{(\mathbb{P}[z_j = 0, \tilde{z}_j = 1] + \mathbb{P}[z_j = 1, \tilde{z}_j = 0])} \mathbb{E}[(f(\mathbf{z}_1^{(j)}) - f(\tilde{\mathbf{z}}_0^{(j)}))^2] \\ &\geq \mathbb{E}[(f(\mathbf{z}_1^{(j)}) - f(\tilde{\mathbf{z}}_0^{(j)}))^2] \end{aligned}$$

Our assumed continuity condition allows us to conclude $\mathbb{E}[\hat{g}^2] \geq \mathbb{E}[\hat{g}_{\text{bitflip-}k}^2]$, and so has uniformly lower variance. For the second bullet, the score function gradient estimator is given by

$$\hat{g}_{R,j} := f(\mathbf{z}) \nabla_\theta \log p_\theta(\mathbf{z}) = f(\mathbf{z}) \left[\frac{1}{\theta_j} z_j - \frac{1}{1 - \theta_j} (1 - z_j) \right]$$

A calculation shows that the expected square is:

$$\begin{aligned} \mathbb{E}[\hat{g}_{R,j}^2] &= \frac{\mathbb{E}[f(\mathbf{z}_1^{(j)})]^2}{\theta_j} + \frac{\mathbb{E}[f(\mathbf{z}_0^{(j)})]^2}{1 - \theta_j} \\ &\geq \mathbb{E}[f(\mathbf{z}_1^{(j)})^2 + f(\mathbf{z}_0^{(j)})^2] \\ &\geq \mathbb{E}[(f(\mathbf{z}_1^{(j)}) - f(\mathbf{z}_0^{(j)}))^2] \end{aligned}$$

where the last line follows when $f \geq 0$ or $f \leq 0$. This shows the lower variance of bitflip- k when compared to Reinforce. We also see that the bound holds with:

$$\mathbb{E}[\hat{g}_{R,j}^2] \geq \frac{1}{\min(\theta_j, 1 - \theta_j)} \mathbb{E}[(f(\mathbf{z}_1^{(j)}) - f(\mathbf{z}_0^{(j)}))^2]$$

and hence, Reinforce is higher variance than bitflip-1 whenever $\min(\theta, 1 - \theta) < \frac{1}{K}$ which implies when $\min(\theta, 1 - \theta) < \frac{1}{2K}$.

(5th bullet point). The 3rd and 4th results come from

$$\begin{aligned}\mathbb{E}[\hat{g}_j^2] &= \frac{1}{(\mathbb{P}[z_j = 0, \tilde{z}_j = 1] + \mathbb{P}[z_j = 1, \tilde{z}_j = 0])} \mathbb{E}\left[\left(f(\mathbf{z}_1^{(j)}) - f(\tilde{\mathbf{z}}_0^{(j)})\right)^2\right] \\ &\geq K \mathbb{E}\left[\left(f(\mathbf{z}_1^{(j)}) - f(\tilde{\mathbf{z}}_0^{(j)})\right)^2\right] \\ &\geq K \mathbb{E}\left[\left(f(\mathbf{z}_1^{(j)}) - f(\mathbf{z}_0^{(j)})\right)^2\right]\end{aligned}$$

where we use the fact that $\mathbb{P}[z_j = 0, \tilde{z}_j = 1] + \mathbb{P}[z_j = 1, \tilde{z}_j = 0] \leq 2 \min(\theta_j, 1 - \theta_j)$ and Assumption 1. Dividing by K on both sides of the inequality leads to the result for the K -sample estimators.

Comparing bitflip-1 to the class of coordinate-wise independent estimators

Theorem 1. Consider a function $f(\mathbf{z}) = \sum_{i=1}^K h(z_i)$. Suppose that an estimator \hat{g} is of the following form:

$$\hat{g}_j = \frac{(-1)^{\tilde{z}_j} \mathbf{1}_{\mathbf{z}_j \neq \tilde{\mathbf{z}}_j}}{p_1(\theta_j) + p_0(\theta_j)} [f(\mathbf{z}) - f(\tilde{\mathbf{z}})] \quad (8)$$

where $p_1(\theta_j) := P[z_j = 1, \tilde{z}_j = 0]$ and $p_0(\theta_j) := P[z_j = 0, \tilde{z}_j = 1]$ and marginally $z_j \sim \text{Bernoulli}(\theta_j)$, $\tilde{z}_j \sim \text{Bernoulli}(\theta_j)$, a general class of estimators which includes DisARM when $p_1(\theta_j) = p_0(\theta_j) = \min(\theta_j, 1 - \theta_j)$ and Reinforce-loo when $p_1(\theta_j) = p_0(\theta_j) = \theta_j(1 - \theta_j)$. Then the following holds:

$$\min_{\theta_1, \dots, \theta_K} \max_{j=1, \dots, K} \text{var}(\hat{g}_j) \geq (K-1)(h(1) - h(0))^2 = \text{var}(\hat{g}_{\text{bitflip-1}})$$

The proof requires the lower bound:

$$\begin{aligned}\text{var}(\hat{g}) &\geq \mathbb{E}[\text{var}(\hat{g} | \mathbf{1}[z_j \neq \tilde{z}_j])] \\ &= \mathbb{E}\left[\mathbf{1}[z_j \neq \tilde{z}_j] \frac{1}{(p_1(\theta_j) + p_0(\theta_j))^2} \sum_{i \neq j} \text{var}(h(z_i) - h(\tilde{z}_i))\right] \\ &= \mathbb{E}\left[\mathbf{1}[z_j \neq \tilde{z}_j] \frac{1}{(p_1(\theta_j) + p_0(\theta_j))^2} \sum_{i \neq j} (h(1) - h(0))^2 (p_1(\theta_i) + p_0(\theta_i))\right] \\ &= \frac{(h(1) - h(0))^2}{p_1(\theta_j) + p_0(\theta_j)} \sum_{i \neq j} (p_1(\theta_i) + p_0(\theta_i))\end{aligned}$$

Now choose j as the one corresponding to one of the smallest values of $p_1(\theta_j) + p_0(\theta_j)$. We have:

$$\begin{aligned}\text{var}(\hat{g}) &\geq ((h(1) - h(0))^2) \sum_{i \neq j} \frac{p_1(\theta_i) + p_0(\theta_i)}{p_1(\theta_j) + p_0(\theta_j)} \\ &\geq ((h(1) - h(0))^2) \sum_{i \neq j} 1 \\ &= (K-1)((h(1) - h(0))^2)\end{aligned}$$

This implies the result of Proposition 5 as a special case of h and \hat{g} . This class of estimators includes the Reinforce-loo estimator when \mathbf{z} and $\tilde{\mathbf{z}}$ are independent and DisARM when \mathbf{z} and $\tilde{\mathbf{z}}$ are antithetic.

When h_i are allowed to have dependence on i we have a weaker result, so long as each h_i is injective. For simplicity of notation assume $p_0(\theta_j) = p_1(\theta_j) =: p(\theta_j)$:

$$\frac{\text{var}(\hat{g}_j)}{\text{var}(\hat{g}_{\text{bitflip},j})} = \frac{1 - 2p(\theta_j)}{2(K-1)p(\theta_j)} + \frac{1}{K-1} \sum_{i \neq j} \frac{p(\theta_i)(h_i(1) - h_i(0))^2}{p(\theta_j)(h_j(1) - h_j(0))^2}$$

Due to the second term there is at least one j such that this variance ratio is at strictly greater than 1 when all $\theta_j \neq 0.5$. Notice that when $2Kp(\theta_j) < 1$ the variance ratio is greater than 1.

Additional Results for P1 and P2

We start by deriving exact variances for the bitflip-1 estimator for these problems. Let $q \sim \text{Categorical}(1, \dots, K)$ be the categorical random variable that selects a coordinate to update. The variance of the j 'th coordinate of the gradient estimate for P1 is then:

$$\begin{aligned} \text{Var}(g_j) &= \text{Var}(K((1-t)^2 - t^2)\mathbf{1}[q=j]) \\ &= K(1-1/K)((1-t)^2 - t^2)^2 \end{aligned}$$

For P2 we have:

$$\begin{aligned} \text{Var}(g_j) &= \mathbb{E}[4K^2 \sum_{i \neq j} \theta_i(1-\theta_i)\mathbf{1}[q=j]] + \text{Var}(2 * K \sum_{i \neq j} \theta_i \mathbf{1}[q=j]) \\ &= 4K \sum_{i \neq j} \theta_i(1-\theta_i) + 4K(1-1/K)(\sum_{i \neq j} \theta_i)^2 \end{aligned}$$

after some cancellation. We can likewise compute exact gradients for the DisARM estimator. For P1 we have:

$$\begin{aligned} \text{Var}(g_j^{\text{DisARM}}) &= E[\text{Var}(g_j^{\text{DisARM}})|\mathbf{1}\{z_j \neq \tilde{z}_j\}] + \text{Var}[E(g_j^{\text{DisARM}})|\mathbf{1}\{z_j \neq \tilde{z}_j\}] \\ &= \frac{1-2\min(\theta_j, 1-\theta_j)}{2\min(\theta_j, 1-\theta_j)}((1-t)^2 - t^2)^2 + \frac{\sum_{i \neq j} \min(\theta_i, 1-\theta_i)}{\min(\theta_j, 1-\theta_j)}((1-t)^2 - t^2)^2 \end{aligned}$$

The presence of the second term comes from the increased expected function differences in DisARM due to antithetic sampling. From the observed expressions for P1, it is readily apparent that bitflip variances are lower whenever $K < \frac{1}{2\min(\theta, 1-\theta)}$ based on the first term alone. On the other hand when θ_i becomes large, though the first term is small the second term (representing differences in the function evaluations) becomes much larger. Consider the case $\theta_i = 0.5$ for all i . The first term in the variance expression becomes 0, but the second term in the variance expression becomes larger, in fact $(K-1)((1-t)^2 - t^2)^2$ the exact variance of bitflip-1. In fact, considering $\theta_j \in [0, 0.5]$ we see that the derivative of the variance with respect to θ_j is negative, so for each θ_j the optimal variance is at $\theta_j = 0.5$. DisARM can thus have lower variance than bitflip-1 when θ_j is near 0.5 but other values θ_i for $i \neq j$ are near the boundary. We consolidate this into a proposition

Proposition 5. *For P1:*

$$\min_{\theta_1, \dots, \theta_K} \max_{j=1, \dots, K} \text{Var}(g_j^{\text{DisARM}}) \geq (K-1)((1-t)^2 - t^2)^2$$

Proof. Without loss of generality we can replace $1 - \theta_j$ with θ_j whenever $\theta_j > 0.5$. As discussed above, if we have $\theta_1 = \dots = \theta_K$, then we have $\frac{\sum_{i \neq j} \min(\theta_i, 1-\theta_i)}{\min(\theta_j, 1-\theta_j)}((1-t)^2 - t^2)^2 = (K-1)((1-t)^2 - t^2)^2$ and so the result holds for all $\theta_1 = \dots = \theta_K$. Otherwise choose the largest θ_i and smallest θ_j so that $\theta_i > \theta_j$. Then $\sum_{k \neq j} \frac{\theta_k}{\theta_j} > K-1$ since $\frac{\theta_k}{\theta_j} \geq 1$ with strict inequality holding for i , which shows the result. This is a special case of Theorem 1.

Choice of τ for UGC

We recommend choosing $\tau \geq \frac{1}{2K}$ in all settings, with $\frac{1}{2K}$ guaranteeing lower variance than the family of estimators (Eq. 3-4) containing DisARM and Reinforce-loo as extremes (contingent on assumption 1). In cases where Assumption 1 holds weakly or does not hold (in the sense that \mathbf{z} close to $\tilde{\mathbf{z}}$ being close does not guarantee closeness of $f(\mathbf{z})$ close to $f(\tilde{\mathbf{z}})$) we recommend using $\frac{1}{2K}$. Such cases include VAEs where f may involve a complex encoder function with no such continuity guarantees. We observe empirically that for VAEs, bitflip-1 gradients are quite high variance when parameter values are far from the boundary (Figure 8-9). On the other hand for functions that (loosely speaking) have such a continuity property such as that of the best subset regression problem, we expect bitflip-1 gradients to have low variance and suggest setting τ in (0.1, 0.33). For this problem we observe robustness to the choice of τ . Future work may formally define classes of functions with varying degrees of continuity and analyze optimal estimators for each case.

P1 Experimental Details

For both P1 and P2, we explore multiple values of t and K . For P1 the learning rate is set to 0.8 and we optimize via projected gradient descent, following standard gradient updates and then clipping the values of the parameters to the range $[0, 1]$. We run 1000 iterations of gradient descent, at each iteration computing a gradient variance estimate with 100 Monte Carlo simulations for each estimator. Initialization is via standard logistic normal distribution. For UGC, τ is set to $\frac{1}{2K}$. We report additional results for varying values of t (Figure 10) and K (Figure 11). Variances are clipped to 10,000 when greater than 10,000 (only applied to DisARM and Reinforce-loo variance) and smoothed with a moving average of window size 20. Either log variance or variance is reported and indicated on y axes, depending on which scale gives higher interpretability.

P2 Experimental Details

To increase variety of settings tested, for P2 we use parameterization by logits $\theta = \frac{e^\phi}{1+e^\phi}$ and hence no longer have a projection step in gradient descent. We set the learning rate to 2.0 and initialize each θ_j to 0.2 deterministically. For UGC, τ is set to $\frac{1}{5}$ for all settings tested. Gradient variances are estimated with a 1000 sample Monte Carlo estimate (and smoothed in the exact same way as P1). We train for 1000 gradient steps. We report additional results for varying t (Figure 12) and varying K (Figure 13).

Subset Selection Experimental Details

The number of features is fixed to 200, the number of observations is set to 60 and the number of active features (non-zero coefficients) is set to 3 (exactly as in (Yin et al. 2020)). The design matrix is sampled $N(0, I)$ for each row and the non-zero β are set to $[3, 2, 1.5]$ (as in (Yin et al. 2020)). y is sampled $N(x^\top \beta, \sigma^2)$, while λ and σ^2 vary throughout the experiments. We train with projected gradient descent for 2000 epochs with learning rate 0.01 in all experiments. We initialize each coefficient $\hat{\beta}$ at 0.1 for all experiments. Due to long training times we estimate the gradient variances with a smaller 5 sample Monte Carlo estimate and apply moving average smoothing, as before. The complete set of results for varying λ and σ^2 are in Figures 14 and 15. UGC is applied with τ set to 0.33. The TPR and FPR on held out data are given in Tables 3 and 4.

Gaussian Mixture Model Experimental Details

We generate samples from a 20-dimensional Gaussian mixture model distribution with 6 components by first sampling component means from a $N(0, 8^2)$ distribution, then sampling data conditional on component means from a Normal distribution with variance σ^2 , with σ^2 being the parameter controlling the signal to noise ratio. For each of the cluster, 100 datapoints are sampled. The encoder and decoder architectures are 2-layer neural networks with a 25-dimensional intermediate layer, with Relu nonlinearities and 0.1 dropout. Optimization is via Adam optimizer with learning rate 0.01, trained for 1000 epochs. Gradient variances are estimated with a 100-sample Monte Carlo estimate at the end of every epoch. Variances are clipped at $10e7$ (only for DisARM and Reinforce-loo) before a moving average is applied with window size 30.

Results on variational autoencoders: FashionMNIST, DynamicMNIST and Omniglot

We repeat the experiment on DynamicMNIST, FashionMNIST and Omniglot of (Dong, Mnih, and Tucker 2020) with latent dimension set to 30 and random normal initialization of all parameters $N(0, 0.3^2)$. We train with learning rates of $1e-3$ for the encoder and decoder and $1e-2$ for the prior variables. The detailed description of model and experiment can be found in (Dong, Mnih, and Tucker 2020). The results across all settings tested appear in Figure 8 and Figure 9.

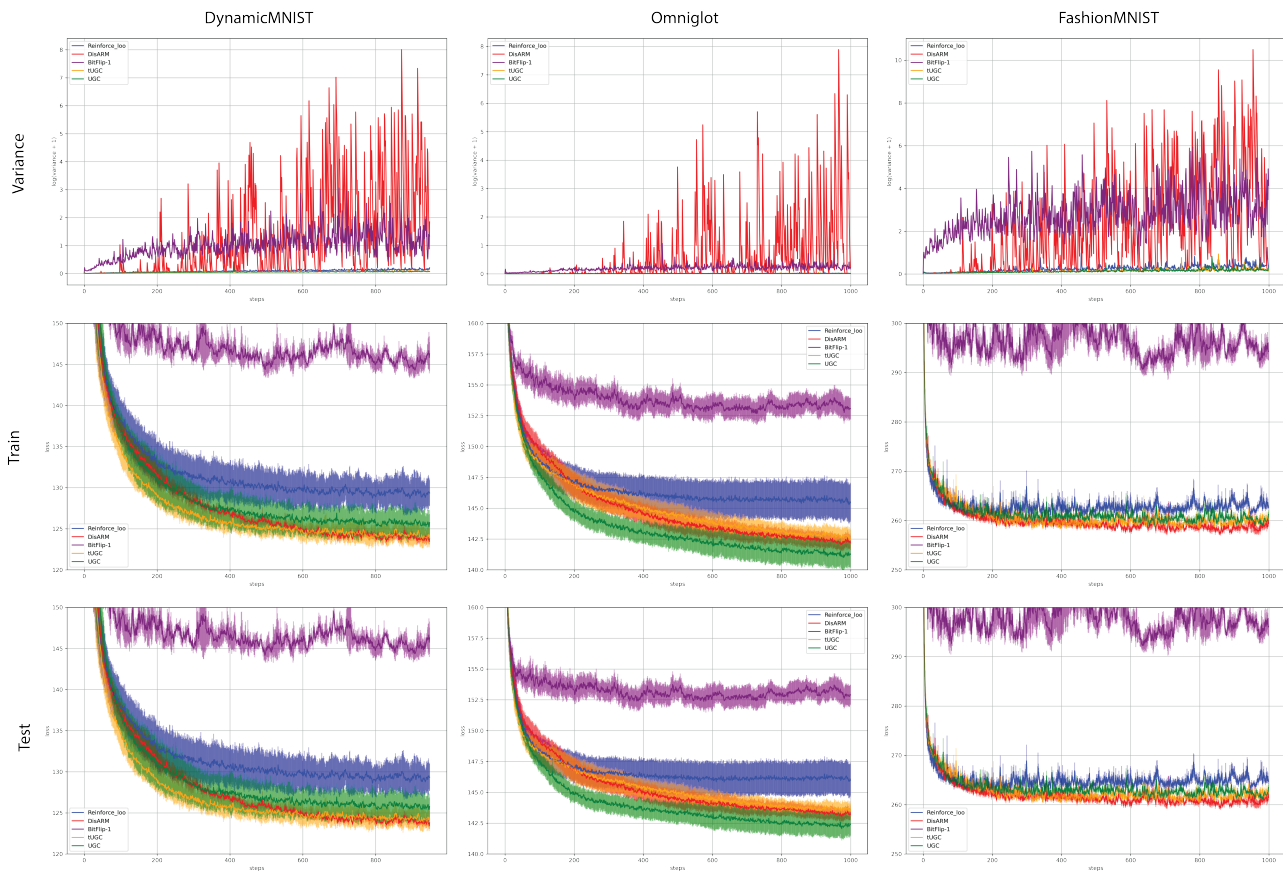


Figure 8: Experiment on VAE with nonlinear encoder and decoder on Dynamic MNIST, FashionMNIST, and Omniglot datasets

Subset selection accuracy for threshold $\theta > 0.5$

$\lambda = 1$

SNR	bitflip-1				UGC				DisARM				Reinforce-loo			
	TPR		FPR		TPR		FPR		TPR		FPR		TPR		FPR	
15.25	0.96	(0.1)	0.0	(0.0)	0.96	(0.1)	0.0	(0.0)	0.56	(0.26)	0.05	(0.02)	0.6	(0.36)	0.04	(0.01)
3.81	1.0	(0.0)	0.0	(0.0)	1.0	(0.0)	0.0	(0.0)	0.66	(0.26)	0.06	(0.03)	0.53	(0.16)	0.04	(0.01)
1.69	0.83	(0.27)	0.01	(0.01)	0.87	(0.22)	0.01	(0.01)	0.43	(0.26)	0.06	(0.03)	0.50	(0.31)	0.05	(0.02)
0.95	0.43	(0.30)	0.04	(0.01)	0.67	(0.21)	0.03	(0.01)	0.40	(0.29)	0.06	(0.02)	0.43	(0.21)	0.05	(0.01)

Table 3: Results on projected gradient descent best subset regression problem for varying signal to noise ratios (SNR), defined as $\beta^T \beta / \sigma^2$. Rounded to 2 decimal places. The number of features $p = 200$, while the active set of features is size 3. The number of observations $n = 60$. UGC achieves the highest performance across settings

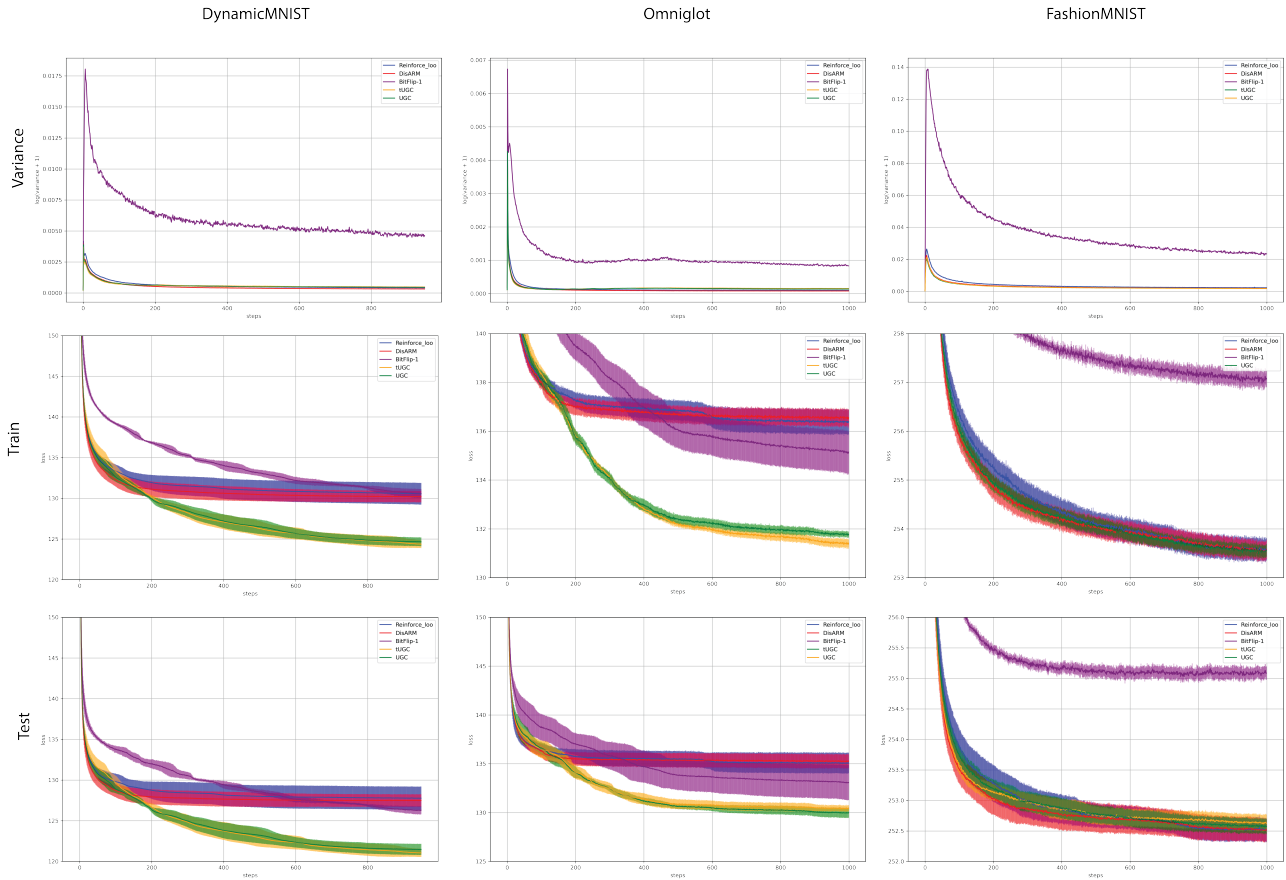


Figure 9: Experiment on VAE with linear encoder and decoder on Dynamic MNIST, FashionMNIST, and Omniglot datasets

Subset selection accuracy for threshold $\theta > 0.5$

SNR = 3.81

λ	bitflip-1				UGC				DisARM				Reinforce-100			
	TPR		FPR		TPR		FPR		TPR		FPR		TPR		FPR	
0.01	0.30	(0.31)	0.31	(0.01)	0.53	(0.27)	0.34	(0.03)	0.83	(0.22)	0.34	(0.02)	0.83	(0.17)	0.31	(0.03)
0.1	0.73	(0.29)	0.11	(0.07)	0.97	(0.10)	0.10	(0.06)	0.83	(0.17)	0.08	(0.03)	0.87	(0.16)	0.08	(0.03)
1.0	0.93	(0.13)	0.0	(0.0)	0.93	(0.13)	0.0	(0.0)	0.47	(0.27)	0.06	(0.02)	0.60	(0.33)	0.05	(0.02)
10.0	0.10	(0.15)	0.0	(0.0)	0.10	(0.15)	0.0	(0.0)	0.50	(0.31)	0.30	(0.03)	0.23	(0.26)	0.33	(0.01)

Table 4: Results on projected gradient descent best subset regression problem for varying λ . Rounded to 2 decimal places. The number of features $p = 200$, while the active set of features is size 3. The number of observations $n = 60$. UGC achieves the highest performance across settings

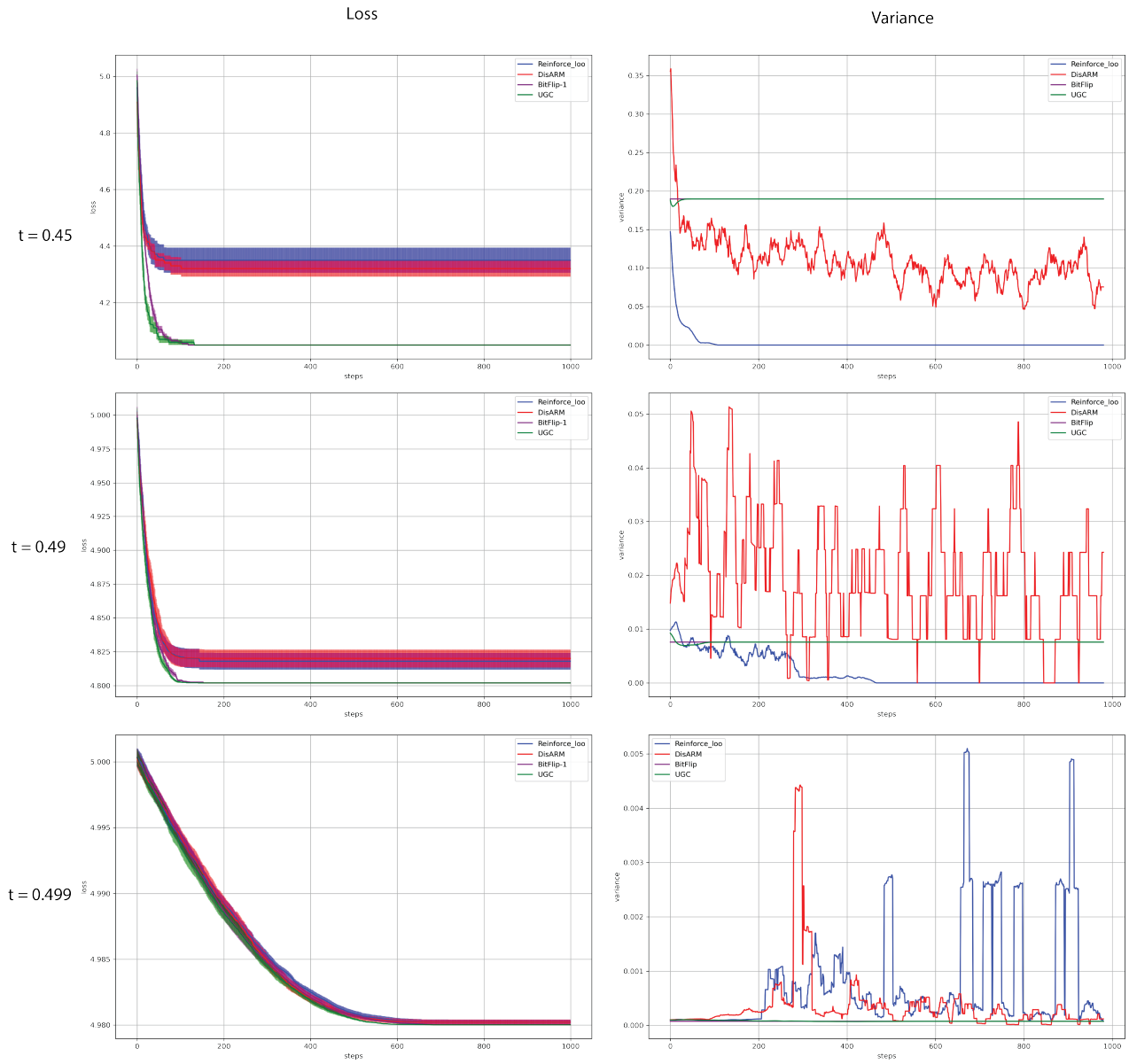


Figure 10: Additional experiments for P1 with varying values of t

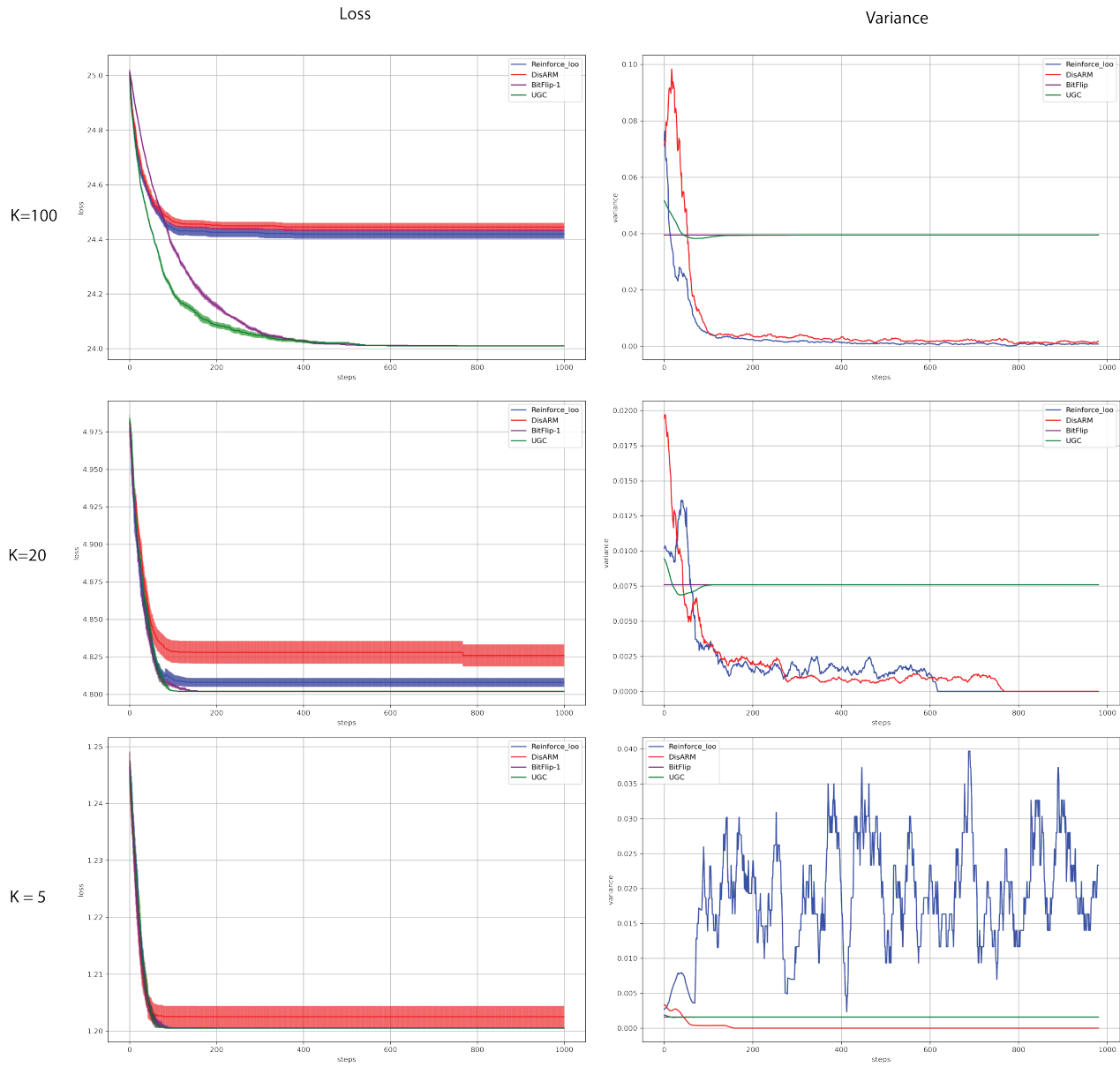


Figure 11: Additional experiments for P1 with varying values of K

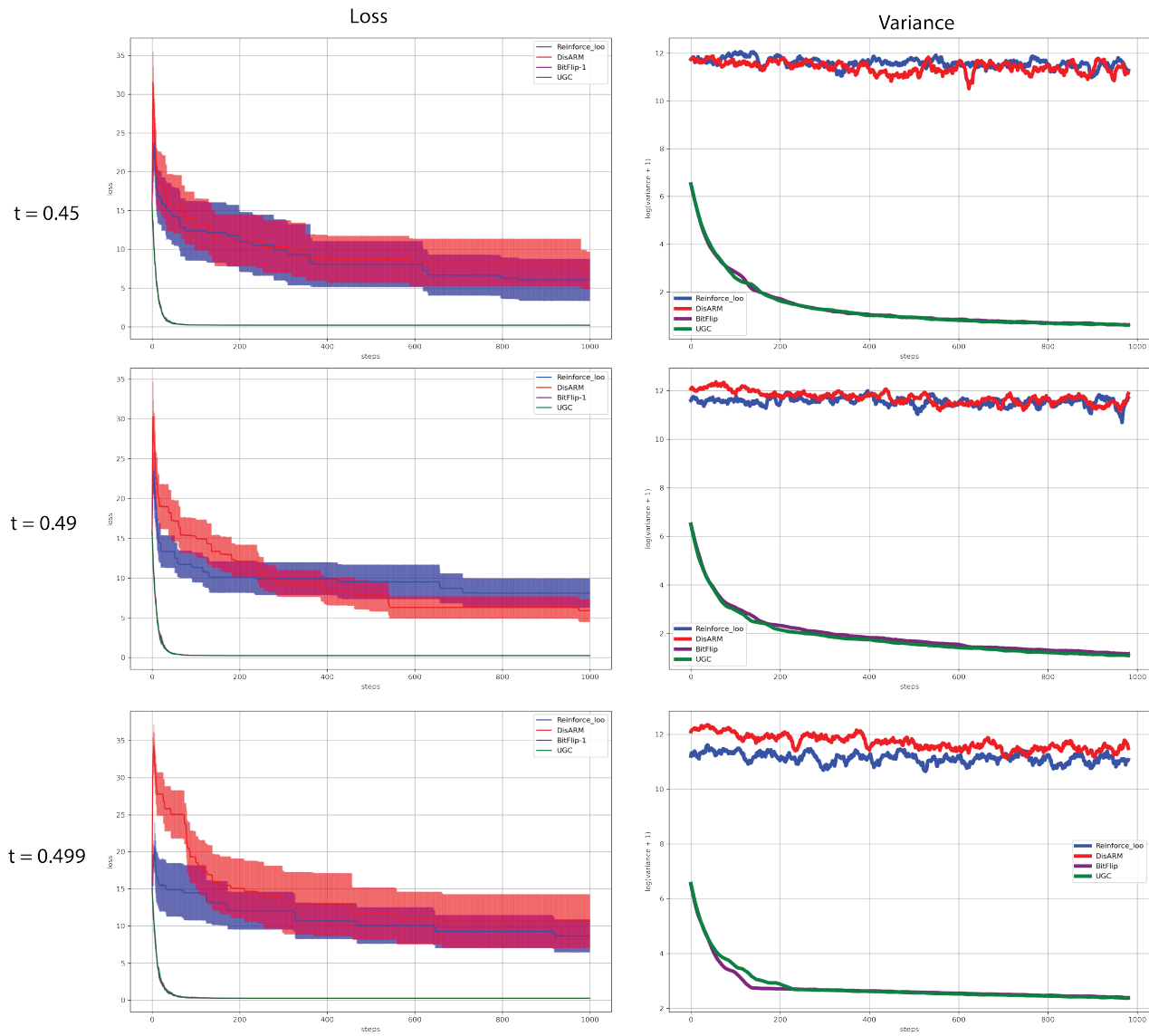


Figure 12: Additional experiments for P2 with varying values of t

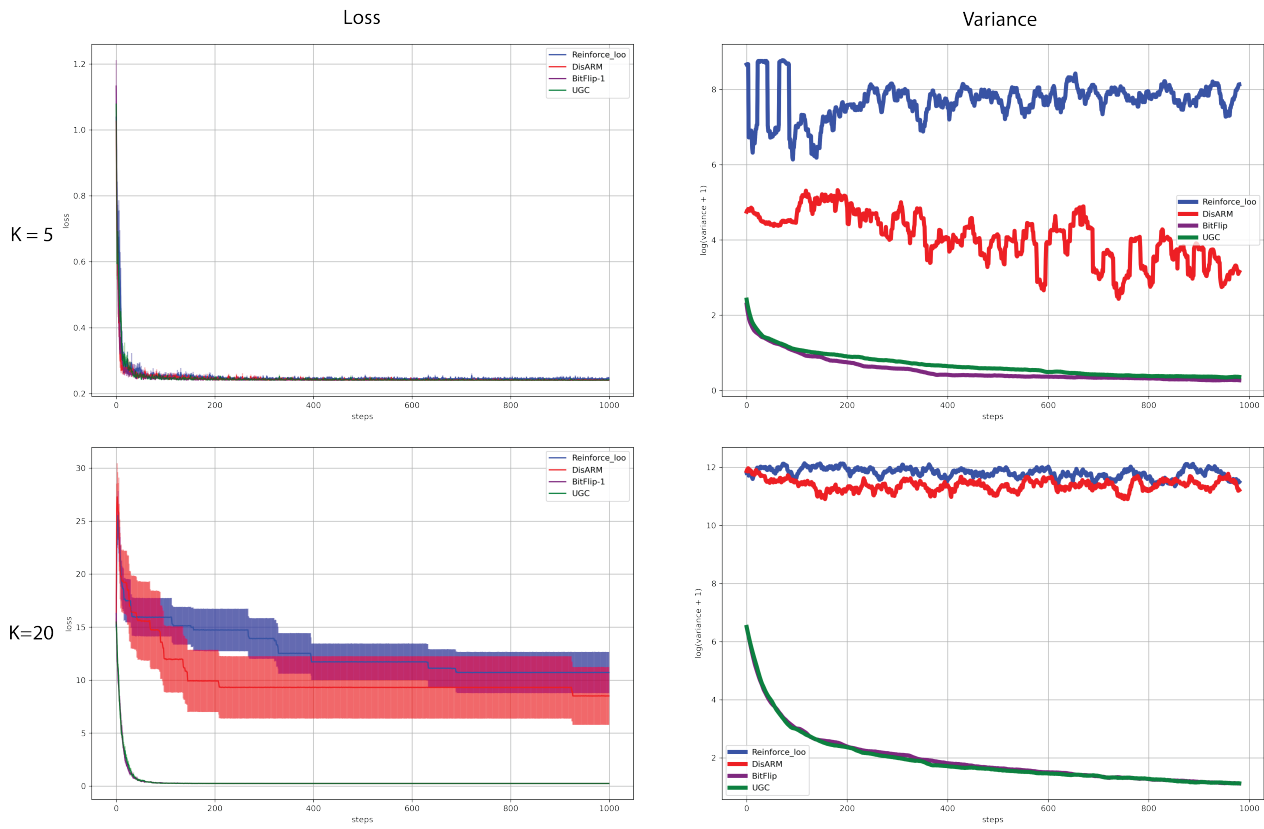


Figure 13: Additional experiments for P2 with varying values of K

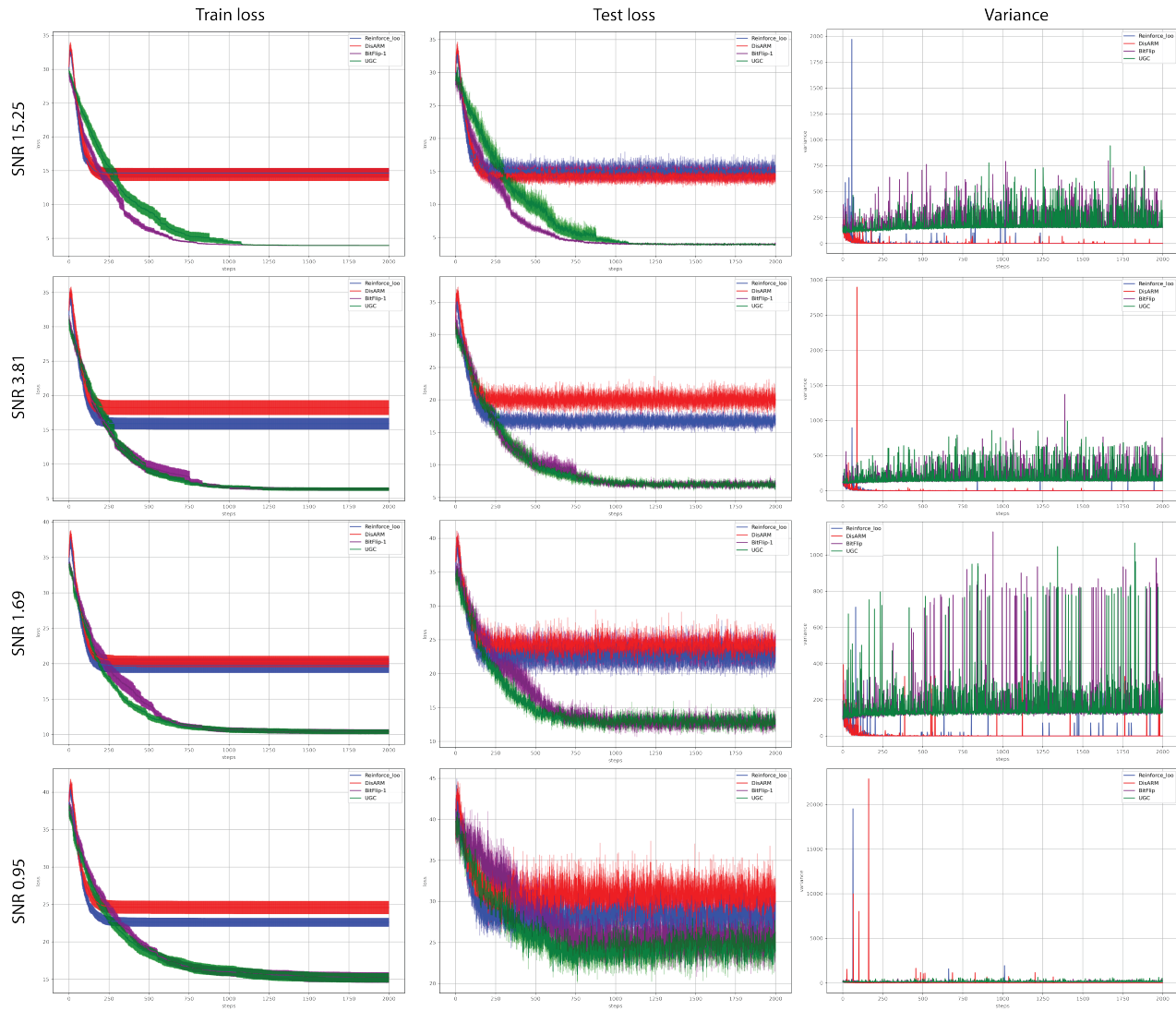


Figure 14: Additional experiments for the best subset selection linear regression problem for varying levels of signal to noise ratio; using projected gradient descent. Low signal to noise ratio generally does not affect convergence (left plots) but affects solution quality as measured by the loss on newly simulated data (middle). On the right, we see that DisARM and Reinforce-top experience high gradients early in training; however, quickly converge to the wrong solution, at which point they become stuck and thereafter have low variance gradients

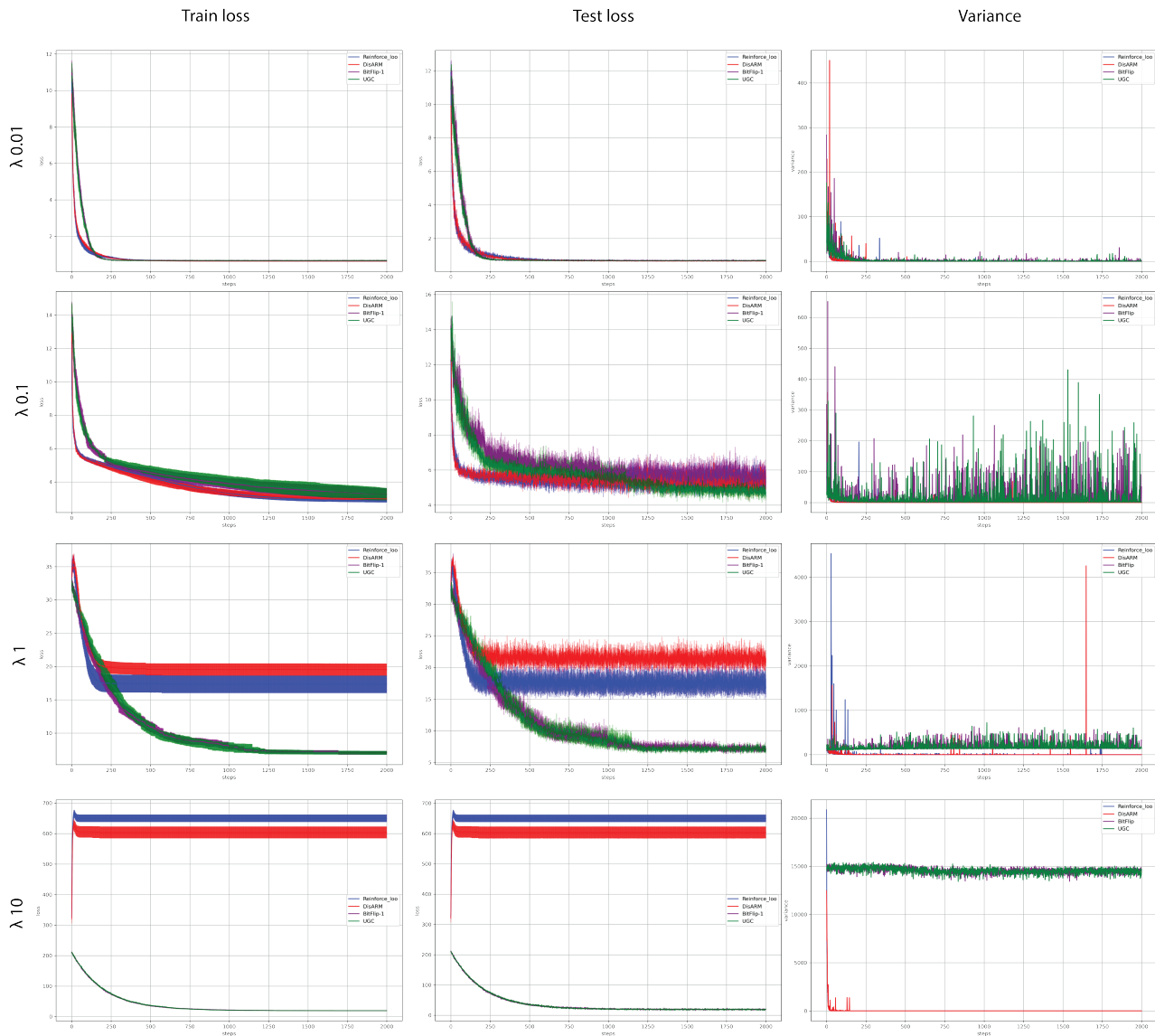


Figure 15: Additional experiments for the best subset selection linear regression problem for varying levels of tuning parameter λ ; using projected gradient descent. At low values of λ all methods converge, with DisARM and Reinforce-loo performing favorably. However at high values of λ DisARM and Reinforce-loo converge to an incorrect solution (bottom rows). This reinforces the idea that the estimators have different behaviors for different functions